(12)

CR 83.004

NAVAL CIVIL ENGINEERING LABORATORY
Port Hueneme, California

Sponsored by
NAVAL FACILITIES ENGINEERING COMMAND

VORTEX SHEDDING FROM CABLES AND STRUCTURES IN A SHEAR FLOW: STATE-OF-THE-ART

November 1982

An Investigation Conducted by
MARINE TECHNOLOGY DIVISION
Naval Research Laboratory
Washington, DC

N68305-82-WR-20092

Approved for public release; distribution unlimited

METRIC CONVERSION FACTORS

Approximate Conversions to Metric Measures

Symbol	When You Know	Multiply by	To Find	Symbol
		LENGTH		
in	inches	*2.5	centimeters	cm
ft	feet	30	centimeters	cm
yd	yards	0.9	meters	m
mi	miles	1.6	kilometers	km
		AREA		
in^2	square inches	6.5	square centimeters	cm^2
ft^2	square feet	0.09	square meters	m^2
yd^2	square yards	0.8	square meters	m^2
mi^2	square miles	2.6	square kilometers	km^2
	acres	0.4	hectares	ha
		MASS (weight)		
oz	ounces	28	grams	g
lb	pounds	0.45	kilograms	kg
	short tons (2,000 lb)	0.9	tonnes	t
		VOLUME		
tsp	teaspoons	5	milliliters	ml
Tbsp	tablespoons	15	milliliters	ml
fl oz	fluid ounces	30	milliliters	ml
c	cups	0.24	liters	l
pt	pints	0.47	liters	l
qt	quarts	0.95	liters	l
gal	gallons	3.8	liters	l
ft^3	cubic feet	0.03	cubic meters	m^3
yd^3	cubic yards	0.76	cubic meters	m^3
		TEMPERATURE (exact)		
°F	Fahrenheit temperature	5/9 (after subtracting 32)	Celsius temperature	°C

*1 in = 2.54 (exactly). For other exact conversions and more detailed tables, see NBS Misc. Publ. 286, Units of Weights and Measures, Price $2.25. SD Catalog No. C13.10:286.

Approximate Conversions from Metric Measures

Symbol	When You Know	Multiply by	To Find	Symbol
		LENGTH		
mm	millimeters	0.04	inches	in
cm	centimeters	0.4	inches	in
m	meters	3.3	feet	ft
m	meters	1.1	yards	yd
km	kilometers	0.6	miles	mi
		AREA		
cm^2	square centimeters	0.16	square inches	in^2
m^2	square meters	1.2	square yards	yd^2
km^2	square kilometers	0.4	square miles	mi^2
ha	hectares (10,000 m^2)	2.5	acres	
		MASS (weight)		
g	grams	0.035	ounces	oz
kg	kilograms	2.2	pounds	lb
t	tonnes (1,000 kg)	1.1	short tons	
		VOLUME		
ml	milliliters	0.03	fluid ounces	fl oz
l	liters	2.1	pints	pt
l	liters	1.06	quarts	qt
l	liters	0.26	gallons	gal
m^3	cubic meters	35	cubic feet	ft^3
m^3	cubic meters	1.3	cubic yards	yd^3
		TEMPERATURE (exact)		
°C	Celsius temperature	9/5 (then add 32)	Fahrenheit temperature	°F

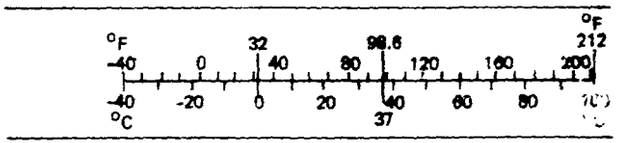

Unclassified

SECURITY CLASSIFICATION OF THIS PAGE (When Data Entered)

REPORT DOCUMENTATION PAGE		READ INSTRUCTIONS BEFORE COMPLETING FORM
1 REPORT NUMBER CR 83.004	2 GOVT ACCESSION NO. AD-A124 864	3 RECIPIENT'S CATALOG NUMBER
4 TITLE (and Subtitle) Vortex Shedding from Cables and Structures in a Shear Flow: State-of-the-Art		5 TYPE OF REPORT & PERIOD COVERED Final; Oct 80 - Aug 82 6 PERFORMING ORG. REPORT NUMBER
7 AUTHOR(s) Owen M. Griffin		8 CONTRACT OR GRANT NUMBER(s) N68305-82-WR-20092
9 PERFORMING ORGANIZATION NAME AND ADDRESS Marine Technology Division Naval Research Laboratory Washington, DC 20375		10 PROGRAM ELEMENT PROJECT, TASK AREA & WORK UNIT NUMBERS PE 62760N YF60.534.091.01.0354
11 CONTROLLING OFFICE NAME AND ADDRESS Naval Civil Engineering Laboratory Port Hueneme, CA 93043		12 REPORT DATE November 1982 13 NUMBER OF PAGES 52
14 MONITORING AGENCY NAME & ADDRESS(if different from Controlling Office)		15 SECURITY CLASS. (of this report) Unclassified 15a DECLASSIFICATION DOWNGRADING SCHEDULE

16 DISTRIBUTION STATEMENT (of this Report)

Approved for public release; distribution unlimited.

17 DISTRIBUTION STATEMENT (of the abstract entered in Block 20, if different from Report)

18 SUPPLEMENTARY NOTES

19 KEY WORDS (Continue on reverse side if necessary and identify by block number)

Cables; Cable strumming; Vortex shedding; Undersea cable structures; Cable dynamics

20 ABSTRACT (Continue on reverse side if necessary and identify by block number)

This report examines the general problem of the flow about bluff bodies in a shear flow in light of the present state of knowledge for these flows, and relates existing studies to the vortex-excited oscillations of slender, flexible structures in air and in water. Experiments with circular cylinders are emphasized, although reference also is made to experiments

DD FORM 1 JAN 73 1473 EDITION OF 1 NOV 65 IS OBSOLETE

Unclassified

SECURITY CLASSIFICATION OF THIS PAGE (When Data Entered)

conducted with cylinders of other cross-sections (D-section cylinders, rectangular cylinders, etc.). Some recent experiments with flexible cables in a shear flow are discussed to the extent possible.

Many of the studies conducted thus far have been limited to cylinders with small aspect ratios or length/diameter less than L/D = 15 to 20. The cellular structure of the vortex shedding is influenced strongly by the end conditions for cylinders with these relatively small values of L/D and so it is important to conduct experiments with cylinders of sufficient length to minimize the effects of the end boundaries. The results obtained from experiments such as these are of particular importance in the design of long, flexible marine structures and cable arrays.

The effects of incident shear on the cross flow response of lightly-damped structures in air and in water should be investigated further. The experiments conducted thus far have demonstrated that cylindrical structures undergo large-amplitude unsteady motions in shear flows when the critical incident flow velocity is exceeded and the damping is sufficiently small. However, more definitive bounds for and details of this fluid-structure interaction are required for applications in both wind engineering design of buildings and structures and ocean engineering design of structures and cable systems.

CONTENTS

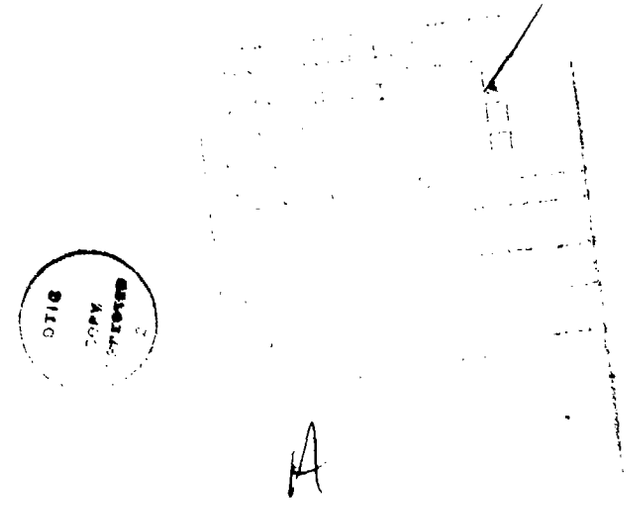

FOREWORD AND ACKNOWLEDGMENTS

This study was conducted at the Naval Research Laboratory as part of an exploratory development program in marine cable dynamics funded by the Naval Civil Engineering Laboratory. Contract research programs to study the effects of shear on vortex shedding from cables and cylinders were conducted at Colorado State University and Virginia Polytechnic Institute and State University. These programs were supported by the NCEL marine cable dynamics program under Navy contracts N68305-78-C-0055 (NCEL) and N00173-80-C-0211 (NRL). A number of helpful comments on the subject matter of the report were made by Professor A. A. Szewczyk of the University of Notre Dame.

EXECUTIVE SUMMARY

The complex fluid-structure interaction associated with vortex shedding from a bluff body in a nonuniform (shear) flow encompasses a wide range of problems. For instance, tall buildings of various cross-sections and slenderness or aspect ratios, i.e., length L/diameter D, often pose difficult and varied problems to the structural designer and architect. These problems include flow-induced structural fatigue and steady loads due to the interaction between the structure and the atmospheric boundary layer. Cylindrical structures such as these are of finite length with a relatively small aspect ratio (L/D = 2 to 15). On the other hand, structures intended for deployment in the ocean range from small aspect-ratio bluff bodies such as marine pilings in relatively shallow water to long cable arrays with aspect ratios of several hundred, to long marine risers, and to pipelines. The cold water intake pipe of an ocean thermal energy conversion (OTEC) power plant also is a long, cylindrical structure deployed in an often nonuniform current field. Ocean currents typically vary vertically and horizontally in both shallow and deep water, so that nonuniform flow effects may need to be given serious consideration by the designer of marine structures and cable systems.

The purpose of this report is to examine the general problem of the flow about bluff bodies in a shear flow in light of the present state of knowledge for these flows, and to relate existing studies to the vortex-excited oscillations of slender, flexible structures in air and in water. Experiments with circular cylinders are emphasized, although reference also is made to experiments conducted with cylinders of other cross-sections (D-section cylinders, rectangular cylinders, etc.). Some recent experiments with flexible cables in a shear flow are discussed to the extent possible.

Many of the studies conducted thus far have been limited to cylinders with small aspect ratios of length/diameter less than L/D = 15 to 20. The cellular structure of the vortex shedding is influenced

strongly by the end conditions for cylinders with these relatively small values of L/D and so it is important to conduct experiments with cylinders of sufficient length to minimize the effects of the end boundaries. The results obtained from experiments such as these are of particular importance in the design of long, flexible marine structures and cable arrays.

It is important also to investigate further the effects of incident shear on the cross flow response of lightly-damped structures in air and in water. The experiments conducted thus far have demonstrated that cylindrical structures undergo large-amplitude unsteady motions in shear flows when the critical incident flow velocity is exceeded and the damping is sufficiently small. However, more definitive bounds for and details of this fluid-structure interaction are required for applications in both wind engineering design of buildings and structures and ocean engineering design of structures and cable systems.

VORTEX SHEDDING FROM CABLES AND STRUCTURES IN A SHEAR FLOW: STATE OF THE ART

1. INTRODUCTION

If a fluid is in relative motion past a stationary bluff, or unstreamlined, structure and the vortex shedding frequency approaches one of the natural frequencies of the structure, then resonant flow-induced oscillations of the cylinder can occur when the damping of the system is sufficiently low. These resonant oscillations are accompanied by a 'lock-on' or capture of the vortex shedding frequency by the vibration frequency over a range of flow speeds, and this lock-on effect causes the wake and the structure to oscillate in unison. The periodic lift and the mean drag forces are amplified as a result of these vibrations, and changes in these fluid forces are closely related to the changes that occur in the flow field in the near wake of the body. Many practical situations involve lightly-damped structures that are located in flows of air or water that are nonuniform along the length of the structure. The primary difference between a uniform flow and a shear flow is the presence and added complexity, in a shear flow, of vorticity whose vector is normal to the plane of the flow. When the incident flow approaches the body this vorticity is turned into the flow direction and it interacts with the vortices which are shed from the body into the wake.

The complex fluid-structure interaction associated with vortex shedding from a bluff body in a nonuniform (shear) flow encompasses a wide range of problems. For instance, tall buildings of various cross-sections and slenderness or aspect ratios, i.e., length L/diameter D, often pose difficult and varied problems to the structural designer and architect. These problems include flow-induced structural fatigue and interactions between the structure and the atmospheric boundary layer. Cylindrical structures such as these are of finite length with a relatively small aspect ratio (L/D = 2 to 15). On the other hand, structures intended for deployment in the ocean range from small aspect-ratio bluff bodies such as marine pilings in relatively shallow water to long cable arrays with aspect ratios of several

hundred, to long marine risers, and to pipelines. The cold water intake pipe of an ocean thermal energy conversion (OTEC) power plant also is a long, cylindrical structure deployed in an often nonuniform current field. Ocean currents typically vary vertically and horizontally in both shallow and deep water, so that nonuniform flow effects may need to be given serious consideration by the designer of marine structures and cable systems. A linear shear flow often is representative of sites where deepwater drilling and exploration are conducted.[†]

The purpose of this report is to examine the general problem of the flow about bluff bodies in a shear flow in light of the present state of knowledge for these flows, and to relate existing studies to the vortex-excited oscillations of slender, flexible structures in air and in water. Experiments with circular cylinders are emphasized, although reference also is made to experiments conducted with cylinders of other cross-sections (*D*-section cylinders, rectangular cylinders, etc.). Some recent experiments with flexible cables in a shear flow are discussed to the extent possible.

2. RELATED INVESTIGATIONS

A number of papers which treat various aspects of unsteady flow phenomena and, in particular, the vortex-excited oscillations of bluff bodies and the equivalent forced vibrations have recently appeared. These include the proceedings of two international symposia on flow-induced structural vibrations (1,2), which contain papers ranging from basic laboratory and analytical studies of vortex formation in uniform and nonuniform flows to field studies of the vibrations of offshore structures. Sarpkaya (3) has reviewed the basic characteristics of vortex shedding and vortex-excited oscillations and has provided one hundred and thirty-four references through early 1979. More recently Griffin and Ramberg (4) have reviewed the same problems in the context of marine applications.

Vortex-excited oscillations are a complex phenomenon when the incident flow to the structure is uniform and steady, but they are even more complex when the structure is at yawed incidence and/or the flow is nonuniform. The former problem of flow at yawed incidence was studied recently by

[†]T. N. Gardner and M. W. Cole, Jr., "Deepwater Drilling in a High Current Environment," Offshore Technology Conference Paper OTC 4316, May 1982.

Ramberg (5), and the latter problem is discussed here. In an early study of shear flow past bluff bodies, Masch and Moore (6) undertook an experimental investigation of the drag force variation on cylinders in the presence of a linear velocity profile at incidence; up to 40 percent deviations from the uniform flow values of the drag coefficient were measured in the case of the linear velocity profile. Visualization of the flow in the wake showed the presence of appreciable secondary flow effects due to the velocity gradient. Starr (7) and Shaw and Starr (8) measured the flow about and the force distribution on circular cylinders in nonuniform flows of water and air. These studies showed the potential importance of characterizing the nonuniform flow in terms of a "steepness parameter" for the incident velocity gradient. Both studies were mainly concerned with identifying design guidelines for use in engineering practice. The steepness parameter is defined by

$$\bar{\beta} = \frac{D}{V_{REF}} \frac{dV}{d\bar{z}} \tag{1}$$

where the velocity gradient is given by $dV/d\bar{z}$ and the cylinder diameter or representative transverse dimension by D. The reference velocity V_{REF} is usually representative of the mid-span incident velocity on a finite-length body or is equal to the velocity at the center of the wind tunnel or flow channel. Sometimes the maximum velocity in the profile is used to define V_{REF}.

A number of investigators have attempted to study nonuniform flow effects from a basic perspective. These studies have included the measurement of the base pressure and vortex shedding characteristics on D-shaped models which span the working section of a wind tunnel (9, 10, 11), base pressure and vortex shedding from finite-length circular cylinders (12), circular cylinders spanning a wind tunnel section (11) and rectangular cylinders of various aspect ratios in low and high turbulence level incident flows (13,14). Mair and Stansby (11) conducted several experiments with D-section cylinders of $L/D = 24$ and 32. In those early experiments on a relatively long cylinder ($L/D > 20$), a quasi-two-dimensional flow region was observed over an appreciable region of the cylinder ($L \sim 15$ D) when $L/D = 32$ and $\bar{\beta} = 0.0125$.

Stansby (15) has measured the vortex shedding characteristics of circular cylinders which spanned the working section of a wind tunnel both in uniform flow and in an incident linear velocity gradient.

The cylinder was forced to vibrate at various frequencies and amplitudes and the bounds for the 'lock-on' of the vortex shedding to the cylinder vibrations were measured for both uniform and nonuniform incident velocity profiles.

Vickery and Clark (16) studied the structure of the vortex shedding from a slender, tapered circular cylinder in smooth and turbulent shear flows. A three-celled shedding pattern was observed in the smooth uniform flow over the free-ended cylinder with a taper of 4 percent along its length. When the smooth flow was replaced by a turbulent shear flow, the vortex shedding cells of constant frequency were less apparent. The shedding frequency in this latter case varied continuously along the lower two-thirds of the cylinder, but two cell-like regions of constant frequency were present over the upper third.

The effect of a sheared turbulent stream on the critical Reynolds number for a circular cylinder was studied recently by Davies (17). The effect of the highly turbulent shear flow ($\bar{\beta} = 0.18$) was to reduce the critical Reynolds number by a factor of ten, from Re_{crit} (smooth flow) = 2 to 3 × 10^5 to $Re_{crit} \approx 3 \times 10^4$. The overall effect was similar to that produced by a highly turbulent uniform flow of the same intensity ($v'/V \approx 5\%$). Once again a cellular vortex structure was observed along the span of the cylinder. The character and extent of each vortex shedding cell was dependent on local conditions and on the cylinder's relatively small aspect ratio, $L/D = 6$.

Stansby (15) has proposed an approximate method for estimating the spanwise extent to which the vortex shedding locks onto the vibrations of a bluff body in a shear flow. A central argument in Stansby's development is that the wake of an oscillating body behaves according to the concept of universal wake similarity. This means that a Strouhal number can be defined that is independent of the characteristic dimensions and flow separation conditions of the body. Griffin (18) recently has demonstrated that the flow about vibrating bluff bodies behaves in this manner and has shown in addition (19) that the principle is valid for a wide variety of structural cross-sections at Reynolds numbers from 200 to 10^7. Stansby's method is somewhat limited to a rigid cylinder and cannot be extended to the case of

a flexible structure or cable with varying displacement amplitude in the spanwise direction. A new formulation that is valid for these conditions is proposed in Section 5 of this report.

A program of experiments recently was conducted to assess the effects of shear on vortex shedding from smooth and rough cylinders at large Reynolds numbers. The results have been reported by Peltzer and Rooney (20). The experiments were conducted with a cylinder of aspect ratio $L/D = 16$ at Reynolds numbers in the range of 1.5×10^5 to 3×10^5 in order to assess the minimum shear (as denoted by the shear parameter $\bar{\beta}$ given above) at which the characteristic lengthwise cellular vortex shedding pattern was initiated. An incipient cellular pattern of vortex shedding was observed at the weakest shear gradient, $\bar{\beta} = 0.007$, and persisted in stronger form over the test range to shear levels given by $\bar{\beta} = 0.04$. Most of the test runs, however, were carried out at values of the shear parameter, $\bar{\beta} = 0.007$ to 0.02, which are representative of full-scale marine and atmospheric site conditions. The results obtained by Peltzer and Rooney provide a reasonably wide data base of circumferential mean pressure and vortex shedding frequencies for smooth and rough circular cylinders at subcritical, critical and supercritical Reynolds numbers.

Experiments to study the effects of a linear shear flow on the vortex shedding from circular cylinders have been conducted by Peterka, Cermak and Woo (21,22). The aspect ratios of the cylinders ranged from $L/D = 12$ to 128 over a Reynolds number range from $Re = 700$ to 8000. Wake frequency spectra, base pressures and wake widths downstream from stationary cylinders were measured for steepness parameters from $\bar{\beta} = 0.016$ to 0.064, and similar experiments were conducted with stationary and vibrating model cables over a range of steepness parameters from $\bar{\beta} = 0.012$ to 0.128.

Peltzer and Rooney (23) recently have measured the vortex shedding patterns on high aspect ratio ($L/D = 27$ and 48) smooth and roughened cylinders in subcritical Reynolds number shear flows. The steepness parameters of the linear shear varied from $\bar{\beta} = 0.0025$ to 0.026 at Reynolds numbers from $Re = 2 \times 10^4$ to 1.2×10^5. Measurements were made of the local Strouhal number and the local base pressure C_{Pb}, and of the vortex formation region length l_F and the wake width d_F at several spanwise locations in the shear profile.

Elsner (24) has conducted an experimental study of the flow about a rectangular cylinder in a highly sheared ($\bar{\beta}$ = 0.08 to 0.09) flow. The Reynolds numbers of the experiments ranged from Re_M = 10^4 to 8×10^4. Measurements were made of the vortex formation length, the wake width, the local base pressure coefficient C_{pb}, the drag coefficient C_D, and the local vortex shedding frequency. The smoke wire technique also was employed to visualize the local wake structure produced by the linear shear flow.

Peltzer (25) has examined the flow about a flexible cable in a linear shear flow. The steepness parameter was $\bar{\beta}$ = 0.0053 and the Reynolds number range of the experiments was $1.8 \times 10^4 \leqslant Re_M \leqslant 4 \times 10^4$. Different distributions of spherical bodies were attached to the cable. The vortex shedding pattern along the cable was significantly altered by the spheres.

Kiya, Tamura and Arie (26) have measured the frequency of vortex shedding from circular cylinders in a linear shear flow. However, in contrast to the other studies described here, the axis of the cylinder was normal to the plane of the shear. The Reynolds numbers of the experiments varied from Re = 35 to 1500 and the shear parameter varied from $\bar{\beta}$ = 0 to 0.25. In order to vary the kinematic viscosity of the fluid over as wide a range as possible, the experiments were conducted in a recirculating channel with mixtures of water and glycerine.

The literature relating to nonuniform flow past bluff bodies is relatively sparse as compared to the corresponding uniform flow case. All of the important papers concerned with this complex phenomenon are discussed here and in the next two sections. The major known characteristics of vortex shedding from stationary and vibrating bluff bodies in nonuniform flows, including the effects of body oscillations, are discussed there in further detail.

3. THE CHARACTERISTICS OF SHEAR FLOW PAST STATIONARY BLUFF BODIES

The basic features of shear flow past bluff bodies now are known for certain restricted conditions. These conditions are somewhat limited in that most experiments have been concerned with wind tunnel studies of vortex shedding from stationary *D*-shaped cylinders, rectangular bodies and, in some cases, circular cylinders. Some less basic studies of shear effects on the flow past circular cylinders have been made in water. From these experiments the following general characteristics have emerged:

(i) The vortex shedding from a *D*-shaped bluff body takes place in spanwise cells, with the frequency constant over each cell. The Strouhal number is constant for each cell when it is based on the body diameter and a characteristic velocity. The latter is usually the velocity measured at the body's half-span (9, 10). These findings generally apply to bodies with aspect ratios less than $L/D = 20$.

(ii) The cellular vortex shedding pattern likewise is found for the case of circular and rectangular cylinders spanning a wind tunnel (11, 12, 13, 17, 20). The number of cells, however, seems to be dependent upon the aspect ratio (L/D) of the cylinder, end effects, etc. (11, 13, 17) for cylinders with $L/D < 20$.

(iii) The base pressure or drag force variation along a circular cylinder is dependent on the aspect ratio (L/D) of the body and is highly sensitive to end conditions (11, 12, 16, 17, 20), for $L/D < 20$. The effects of the end condition become more pronounced when the body has a free end and does not completely span the wind tunnel (12,16).

(iv) When the shear flow is highly turbulent ($v'/V \sim 5$ percent or greater), a reduction in the critical Reynolds number by a factor of ten has been observed in the case of a circular cylinder (17). The effects of the linear shear flow in reducing the critical Reynolds number are similar to a uniform flow of high turbulence level. The shear flow "steepness parameter" was $\bar{\beta} = 0.18$ in these experiments; this is considerably greater than the range, $\bar{\beta} = 0.01$ to 0.05, that is typical of most laboratory studies (10, 11, 13, 15). In two other studies of the

flow around a rectangular cylinder (chord W/thickness $D = 0.5$) in a highly turbulent stream ($v/V \sim 10$ percent), the steepness parameter was $\bar{\beta} = 0.09$ to 0.11, also a relatively high value (14, 24). These experiments once again revealed the formation of cells of constant vortex shedding frequency along the body, with the transition from cell to cell taking place over a greater length of the cylinder than for low turbulence shear flows. The peaks in the frequency spectra also were much broader than in the analogous low-turbulence shear flow.

(v) Surface-roughened circular cylinders also exhibit the characteristic cellular vortex shedding pattern in low- and moderate-turbulence shear flows (20). This was observed for both subcritical and supercritical Reynolds numbers, with a wide range of steepness parameters, $\bar{\beta} = 0.007$ to 0.04. Any linear shear (as low as $\bar{\beta} = 0.007$) was found to trigger a cellular vortex shedding pattern over the length of the cylinder with an aspect ratio of $L/D = 16$. A general trend toward decreasing cell length with increasing shear was found along with an increase in the average cell length with cylinder roughness.

(vi) The tendency for cells to form usually is highest for short L/D cylinders and at the end boundaries of cylinders. Experiments with cylinders of long aspect ratio ($L/D = 20$ to 50 and larger) have demonstrated in one case no discernible cell structure away from the end influences at subcritical Reynolds number (23) or in another case a slight and irregular cell structure at high shear levels of $\bar{\beta} > 0.05$ (21). Experiments with a long flexible cable ($L/D \approx 100$) have shown that a discernible cell structure existed at moderate subcritical Reynolds numbers when $\bar{\beta} = 0.005$ (25).

(vii) Shear in the flow incident upon a circular cylinder also has an effect on the vortex shedding when the axis of the cylinder is normal to the plane of the shear profile. However, larger values of the steepness parameter $\bar{\beta}$ are required for the shear to have a discernible effect. The Strouhal number—Reynolds number dependence for $Re < 1000$ essentially was the same in uniform and shear flows for $\bar{\beta} < 0.1$ (26). For $\beta = 0.1$ to 0.25 the shear resulted in an increase of up to 25 percent in the Strouhal number from the corresponding uniform flow.

Some typical results from the studies summarized above now are discussed. Peltzer and Rooney (20) have conducted one of the most complete and up-to-date studies of the effects of shear on vortex shedding from circular cylinders. The Reynolds numbers for their experiments spanned the range from $Re = 1.6 \times 10^5$ to 3.6×10^5, for smooth and roughened cylinders (roughness $\delta/D = 1 \times 10^{-3}$), and steepness parameters from $\bar{\beta} = 0$ (uniform flow) to $\bar{\beta} = 0.041$. This range of parameters was sufficient to provide both subcritical, critical (or transcritical), and supercritical vortex shedding conditions.

Some of the uniform flow baseline conditions for the smooth and rough cylinders are plotted in Fig. 1, along with some recent measurements by Buresti and Lanciotti (27) and by Alemdaroglu, Rebillat and Goethals (28). The three Reynolds number ranges just mentioned are noted in Fig. 1. The critical Reynolds number Re_δ of 200 to 250 is in good agreement with the value of $Re_\delta = 200$ found by Szechenyi (29). It appears that full supercritical conditions are not reached in the range of Re_δ plotted in Fig. 1, since Szechenyi found that St did not become constant again until a range of $Re_\delta = 800$ to 1000 was reached. Alemdaroglu, Rebillat and Goethals also obtained full supercritical conditions as the roughness Reynolds number approached $Re_\delta = 1000$. The supercritical Strouhal numbers measured by Szechenyi were slightly higher ($St \sim 0.26$) than those plotted in Fig. 1.

When shear was added to the incident flow the results were as shown in Fig. 2 for a typical example. The spanwise variation of the Strouhal number at this Reynolds number ($Re = 2.6 \times 10^5$) and steepness parameter ($\bar{\beta} = 0.016$) indicates a two-cell vortex shedding structure with two end plate cells. The frequency spectra and circumferential pressure coefficients plotted by Rooney and Peltzer clearly show this case to be subcritical. At the same steepness parameter, $\bar{\beta} = 0.016$, the rough cylinder exhibited supercritical shedding over the high velocity portion of its length for $Re = 2.6 \times 10^5$, while the remainder of the cylinder over the low velocity portion of the shear profile remained in the critical range.

In one of the earliest studies of shear flow past bluff bodies, Maull and Young (9, 10) conducted wind tunnel experiments to measure the vortex shedding from a D-section cylinder (chord W/thickness $D = 6$) with a blunt base. The cylinder had a length-to-thickness ratio of $L/D = 20$ and was placed in a shear flow with a steepness parameter $\bar{\beta} = 0.025$. The base pressure coefficient C_{pbM} and the Strouhal number St_M based upon the center-line velocity V_M are shown in Fig. 3. The vortex shedding took place in four cells of constant frequency along the span of the cylinder. One cell extends from $\bar{z}/D = 0$ to 6 and the second from $\bar{z}/D = 7$ to 10. The third cell extends from $\bar{z}/D = 10$ to 15 and the last appears at $\bar{z}/D = 16$.

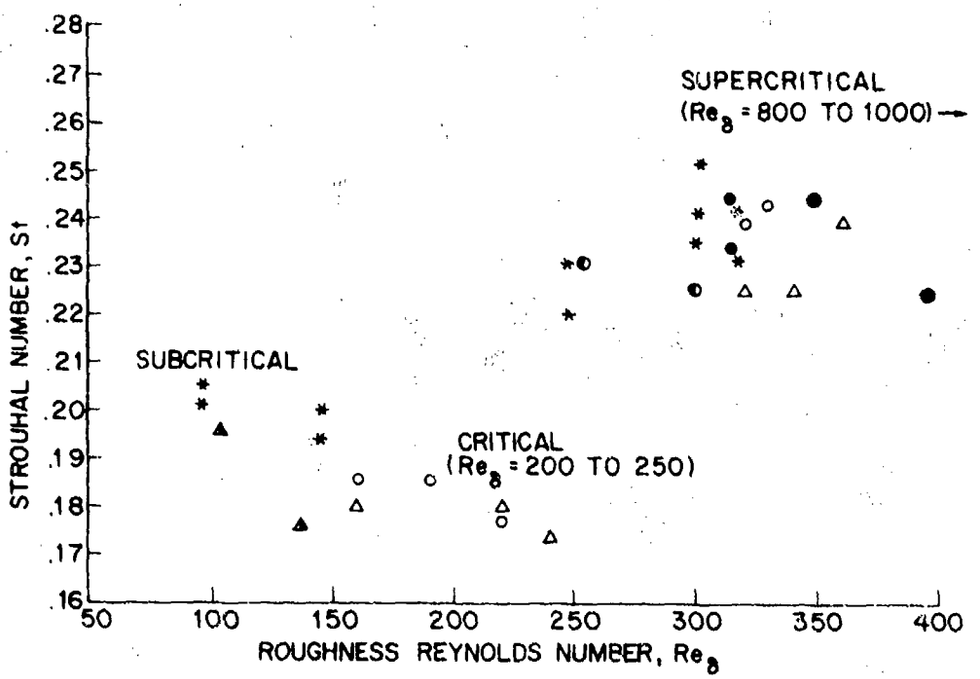

Figure 1. Strouhal number $St = f_s D/V$ plotted against the roughness Reynolds number $Re_\delta = V\delta/\nu$. Here δ is the cylinder surface roughness. Legend for data points:

Peltzer and Rooney (29):
- ○ Rough ($\delta/D = 10^{-3}$)
- △ Rough, low turbulence = .03%

Buresti and Lanciotti (27):
- * Rough ($\delta/D = 10^{-3}$)
- ● Rough ($\delta/D = 3.5 \times 10^{-3}$)

Alemdaroglu, Rebillat and Goethals (28):
- ▲ Rough ($\delta/D = 10^{-3}$)
- ◐ Rough ($\delta/D = 5 \times 10^{-3}$)
- ◑ Rough ($\delta/D = 3.4 \times 10^{-3}$)

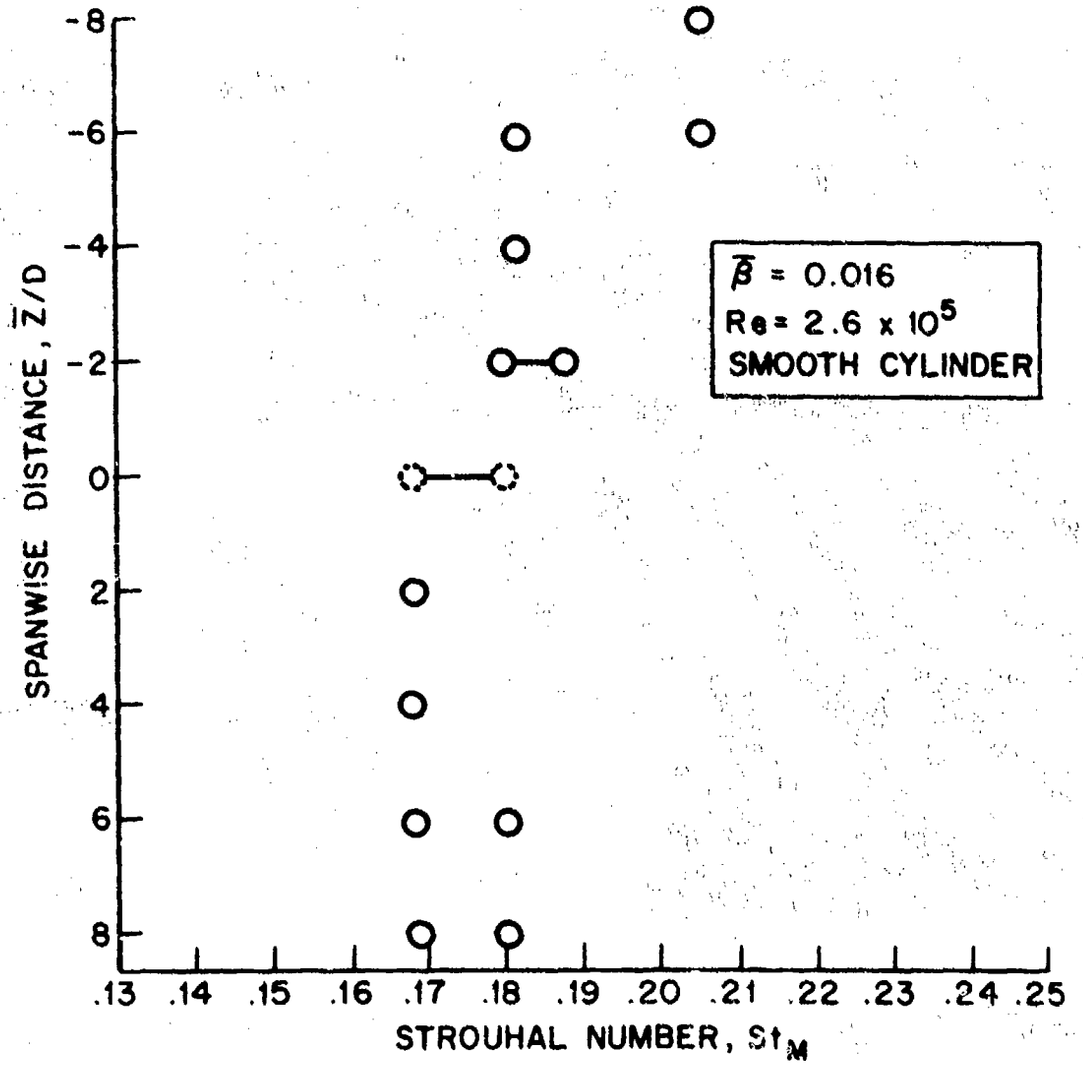

Figure 2. Strouhal number St_M (based upon the center line velocity V_M) plotted against spanwise distance along a circular cylinder in a linear shear flow; from Peltzer and Rooney (20). Reynolds number Re_M = 2.6×10^5; shear flow steepness parameter $\bar{\beta}$ = 0.016.

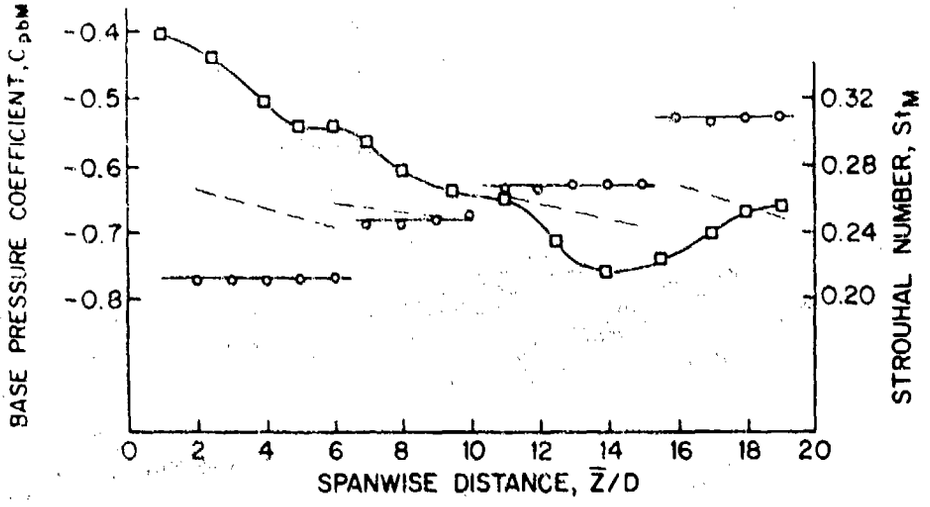

Figure 3. Base pressure coefficient C_{pbM} and Strouhal number St_M (based upon the center line velocity V_M) plotted against the spanwise distance along a D-section cylinder in a linear shear flow; from Maull and Young (10). Reprinted by permission of the Cambridge University Press. Reynolds number $Re_M = 2.8 \times 10^4$; shear flow steepness parameter $\bar{\beta} = 0.025$; cylinder chord/thickness ratio $W/D = 6$.

Frequency spectra recorded by Maull and Young showed that the cell boundary regions ($\bar{z}/D = 7$, as one example) were marked by two characteristic frequencies, one from each of the adjacent cells. The variation of the base pressure in Fig. 3 shows marked changes at the cell boundaries, with noticeable variations in the C_{PbM} versus $\bar{z}/D$ curve at $\bar{z}/D = 6$ and 10. Within each vortex shedding cell the frequency of shedding was constant while the base pressure varied along the span of the cylinder. A study of flow visualization photographs by Maull and Young indicated that the cells were divided by longitudinal vortices aligned with the free-stream direction (10).

The effect of a highly turbulent incident shear flow on the vortex shedding from a circular cylinder was studied by Davies (17). The steepness parameter of the flow was $\bar{\beta} = 0.18$ and the turbulence level was about $v/V = 5$ percent. End plates were fitted to the cylinder at ± 3 D from the center line of the wind tunnel. The base pressure coefficient at the mid-span location on the cylinder is plotted against the Reynolds number in Fig. 4. Also plotted in the figure for comparison are base pressure measurements that had been made in uniform smooth and turbulent flows at the National Physical Laboratory. It is clear that the onset of the critical Reynolds number is reduced in the shear flow by a factor of ten from the uniform smooth flow value of $Re = 2$ to 3×10^5. The reduction in Re_{cri} is similar to that produced by a uniform flow of the same turbulence intensity.

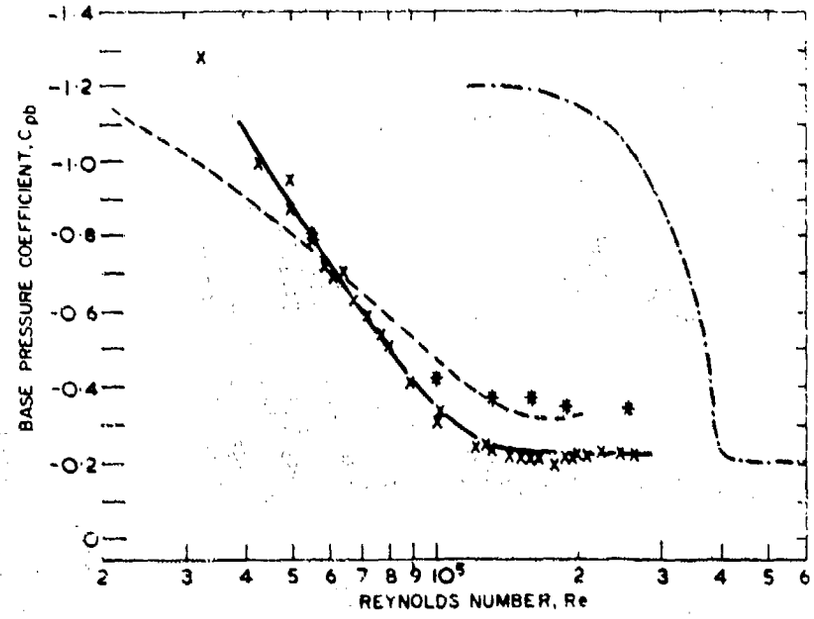

Figure 4. Base pressure coefficient C_{pb} at the center line plotted against the Reynolds number Re_M for a circular cylinder in a shear flow; from Davies (17). Legend for data:

× Center-line value, C_{pbM} ($\bar{\beta} = 0.18$)
— · — Uniform smooth flow
----- Uniform turbulent flow (Bearman 1968)
* Average value ($\bar{\beta} = 0.18$)

Additional measurements of base pressure were made by Davies along the length of the cylinder, for different mid-span Reynolds numbers. For subcritical conditions a well-defined cell structure with a predominant wake frequency and strong vortex shedding was observed. Both the base pressure coefficients based on local velocity and the mid-span value gave a clear picture of the cell boundaries. The shedding patterns became more irregular as the incident flow velocity was increased, and by $Re = 10^5$ any trace of a vortex shedding peak had disappeared into the turbulent background of the frequency spectrum.

Vickery and Clark (16) studied the structure of the vortex shedding from a slender, tapered circular cylinder in smooth and turbulent shear flows at subcritical Reynolds numbers between 2×10^4 and 7×10^4. The cylinder had a base diameter $D = 65$ mm (2.55 in.), a taper of 4 percent, and an aspect ratio of $L/D = 14$. A vortex shedding pattern with three cells of nearly constant frequency was observed in the smooth uniform flow, a finding which is analogous to the case of a uniform cylinder in

a sheared incident flow. When the smooth flow was replaced by a shear flow with a high (4 to 10 percent) turbulence level, a continuous variation of the vortex shedding frequency was observed over the lower two-thirds of the cylinder where large changes took place ($\Delta V / V_{TIP} = 50$ percent) in the incident flow velocity. An apparent cell-like pattern with two constant-frequency cells continued to exist over the upper third of the cylinder near the free end where the incident flow velocity changed very slowly.

Vickery and Clark also measured base pressure, drag and lift coefficients at close intervals along the cylinder. The base pressure coefficient based on the local velocity varied only slightly about $C_{pb} = -0.8$ in smooth flow, but in the turbulent shear flow C_{pb} varied from -0.6 near the cylinder's free end, to -0.9 at half the distance along the cylinder, and to $C_{pb} = -1.05$ near the base. Both the average drag coefficients and base pressures were substantially (25 percent) lower than typical values reported for uniform circular cylinders at the same Reynolds numbers. Based upon their experiments, Vickery and Clark developed a forced vibration, aeroelastic model for predicting small displacement amplitude ($\bar{Y}/D < 0.01$) vortex-excited oscillations. No account was taken of the nonlinear resonance between the structural motion and the cross flow oscillations that is well known at larger displacement amplitudes.

Peterka, Cermak and Woo (21,22) have conducted experiments to study the vortex shedding from large aspect-ratio ($L/D = 12$ to 128), stationary and vibrating circular cylinders and flexible cables in a linear shear flow. Figure 5 shows the Strouhal number based on centerline velocity for the $L/D = 34$, $\bar{\beta} = 0.032$ and $Re = 4000$. This figure confirms the two cells at the boundaries and shows a tendency toward a cellular vortex pattern over the central section of the stationary cylinder. Regions with a similar frequency can be identified over a limited distance, but it is not clear that cells with well-defined boundaries exist. When the data from Fig. 5 are presented as Strouhal numbers based on the local velocity (21), the data are grouped around Strouhal numbers of 0.2 to 0.21. The data indicates a tendency toward a weak cell structure but no clear cell boundaries can be identified in many regions.

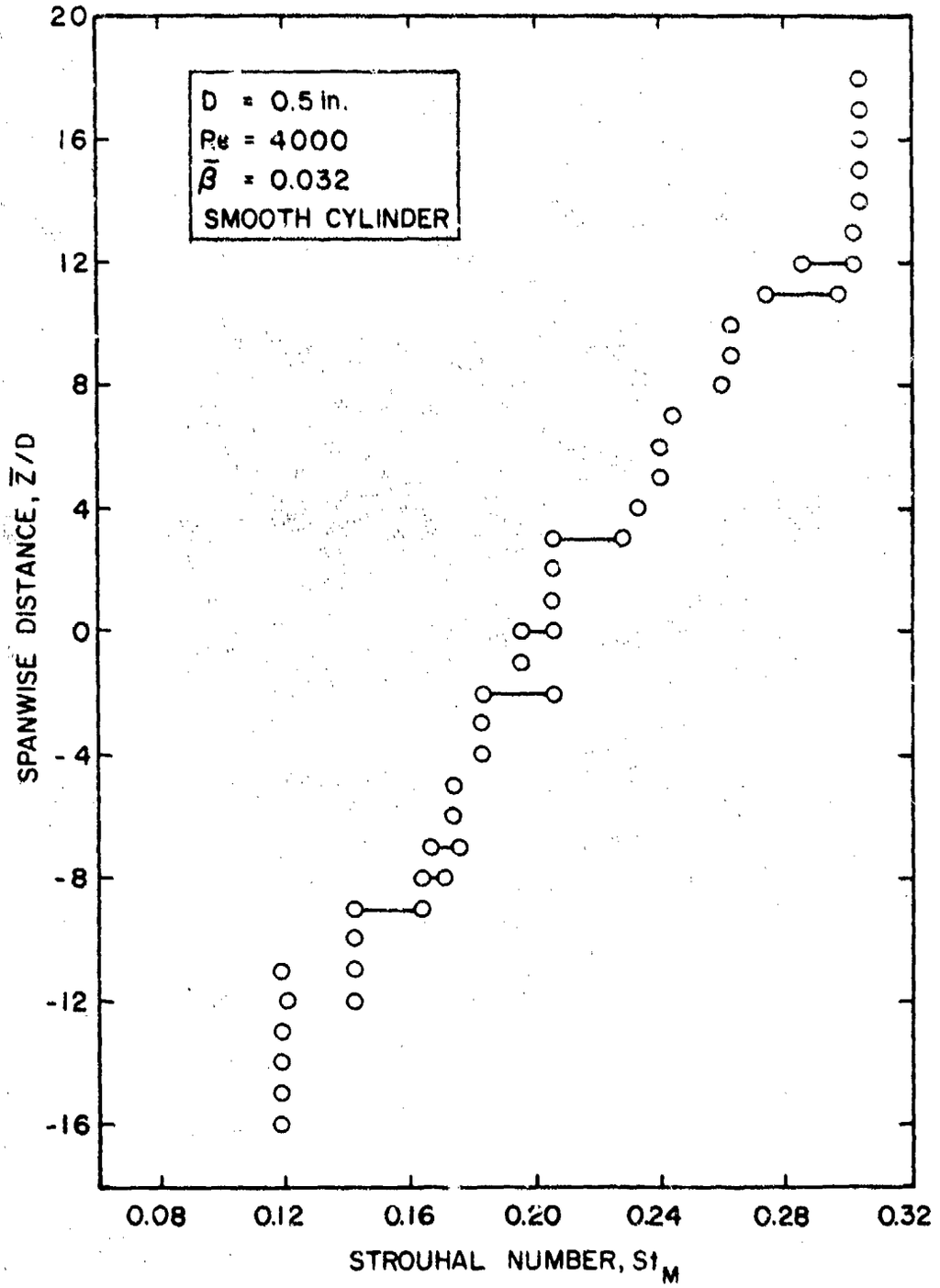

Figure 5. Strouhal number St_M (based upon the center line velocity V_M) plotted against the spanwise distance along a circular cylinder in a linear shear flow; from Peterka, Cermak and Woo (21). Reynolds number $Re_M = 4000$, shear flow steepness parameter $\bar{\beta} = 0.032$

Two smoke visualization photographs of the wake of the same cylinder at a Reynolds number slightly below 2000 are shown in Fig. 6. The region observed is roughly from the centerline to $L = 8$ D below the centerline where no clear indication of a cell structure was evident from frequency measurements in the wake. The smoke was illuminated by a strobe light that was synchronized with the shedding frequency, and an exposure time long enough to cover about six or seven shedding cycles was used. The periodic structure seen in the smoke pattern along the cylinder length is a result of smoke introduction through equally spaced holes in the base of the cylinder. If a coherent cell shedding at the strobe frequency for seven or eight cycles existed during the exposure time, the result would appear as a banded system as seen in the top photograph. If a cell with a frequency different from the strobe frequency was shedding or if no shedding occurred during the exposure time, the result would look like the bottom photo. However, the photos in Fig. 6 were taken at two different times using the same strobe frequency. These results suggest that cells of finite size, but of different frequencies and extent, exist at different times in the wake (21,22). An inclined pattern of vortex shedding similar to that shown in the top photograph was observed by Stansby (15) for a cylinder with $L/D = 16$, $\bar{\beta} \approx 0.025$ and $Re \approx 3000$.

Peltzer and Rooney (23) undertook a study of the effects of shear on vortex shedding from smooth and rough circular cylinders at subcritical Reynolds numbers. Experiments were conducted at $Re \approx 2 \times 10^4$ to 1.2×10^5 and at $\bar{\beta} = 0$ to 0.026. The distribution of the base pressure coefficient $-C_{pb}$ along an $L/D = 48$ cylinder with roughness $k/D = 0.001$ is shown in Fig. 7. This result is typical of the data obtained by Peltzer and Rooney in that end effects were apparent adjacent to the end plates of the cylinder. However, at $|\bar{z}/D| < 16$ no cell pattern was observed and the base pressure varied linearly along the cylinder. A similar linear variation also was measured for the Strouhal number St_{hf}, except for $\bar{z}/D = +4$ to $+8$ where a single cell was observed. In general, the vortex shedding patterns were free of constant frequency cells except for short sections adjacent to the end boundaries.

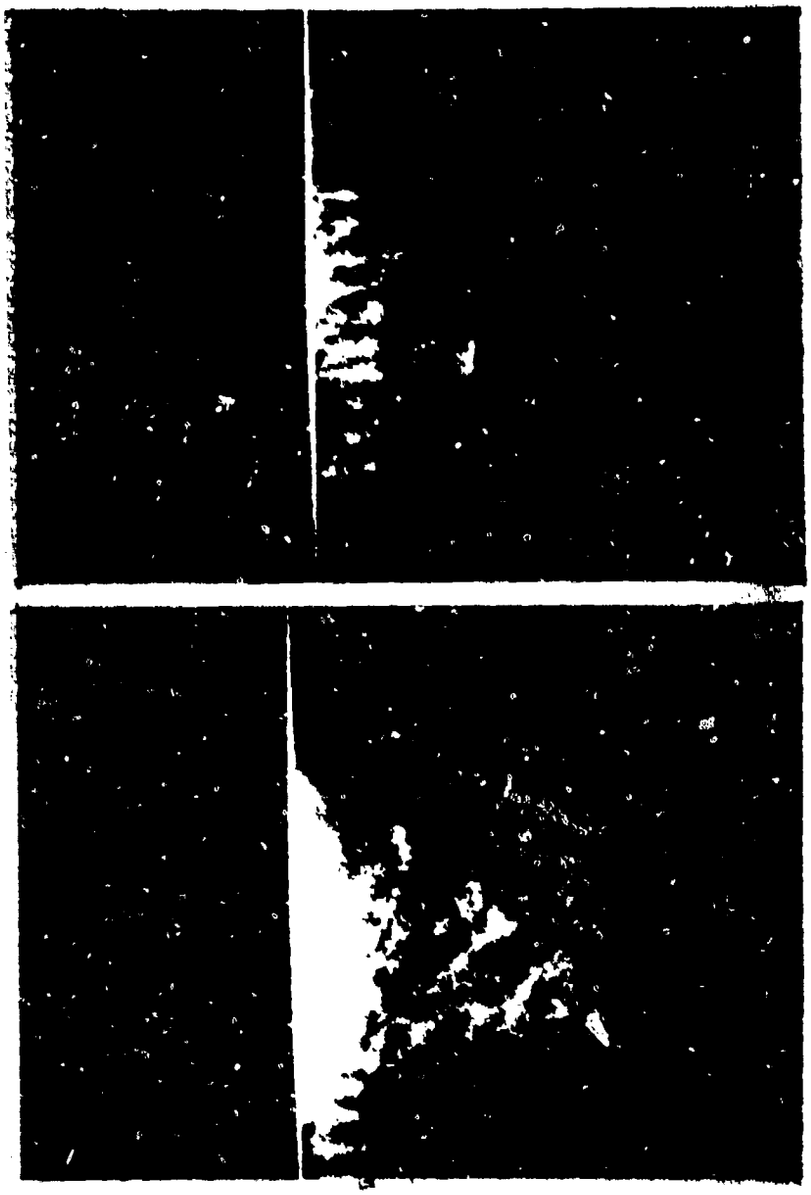

Figure 6. Long exposure photographs of vortex shedding from a circular cylinder in a linear shear flow; from Peterka, Cermak and Woo (21). Reynolds number $Re_M = 2000$; shear flow steepness parameter $\bar{\beta} = 0.032$; cylinder aspect ratio $L/D = 20$. The photographs were provided by Dr. Jon Peterka, Colorado State University.

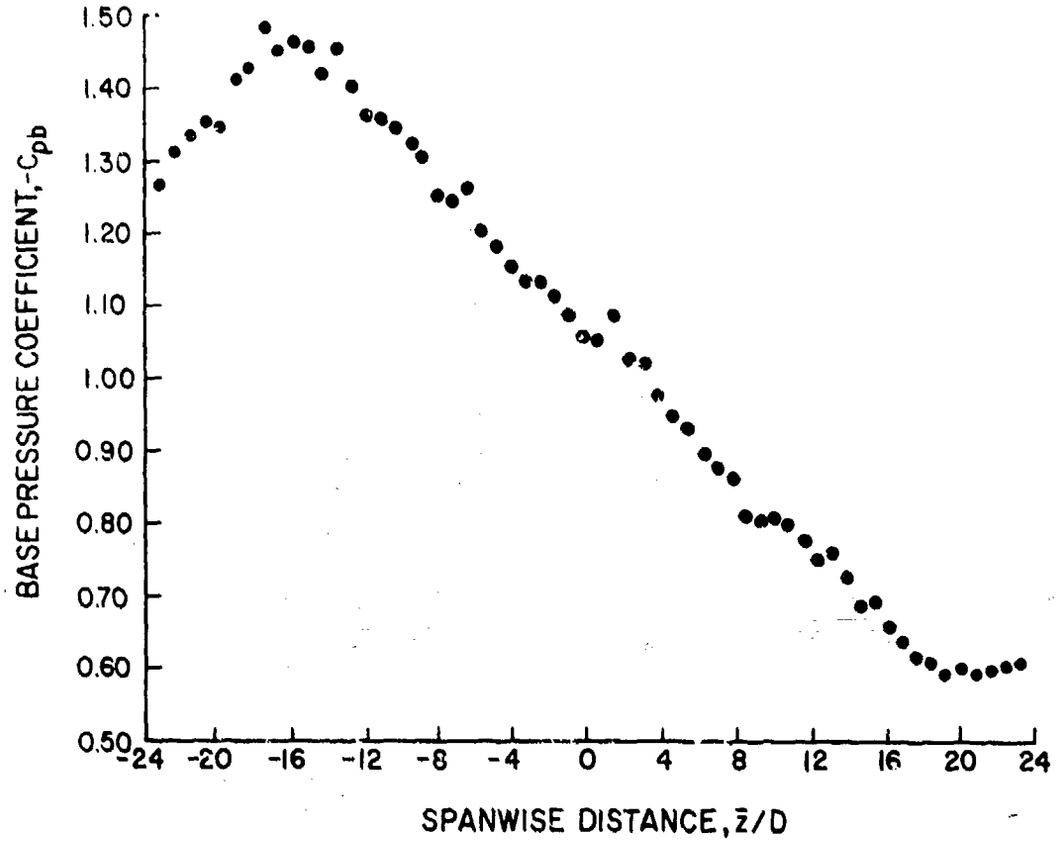

Figure 7. Spanwise variation of the base pressure coefficient C_{Pb} on a rough circular cylinder in a shear flow; from Peltzer and Rooney (23). Reynolds number $Re_M = 2(10^4)$, shear flow steepness parameter $\bar{\beta} = 0.015$.

The experiments conducted by Peltzer and Rooney included simultaneous measurements of the Strouhal number, the base pressure coefficient $-C_{pb}$ and the wake width D'. From these parameters the universal Strouhal number (19)

$$St^* = \frac{f_s D'}{V_s} = \frac{St}{K}\left(\frac{D'}{D}\right)$$

can be estimated. Here $K = V_s/V = \sqrt{1 - C_{Pb}}$ and St is the usual form of the Strouhal number. St^* is plotted against the wake Reynolds number

$$Re^* = \frac{V_s D'}{\nu} = Re\ K\left(\frac{D'}{D}\right)$$

in Fig. 8. The individual data points are calculated from the measurements by Peltzer and Rooney and they are in reasonably good agreement with previous data given by Griffin. The data shown by the

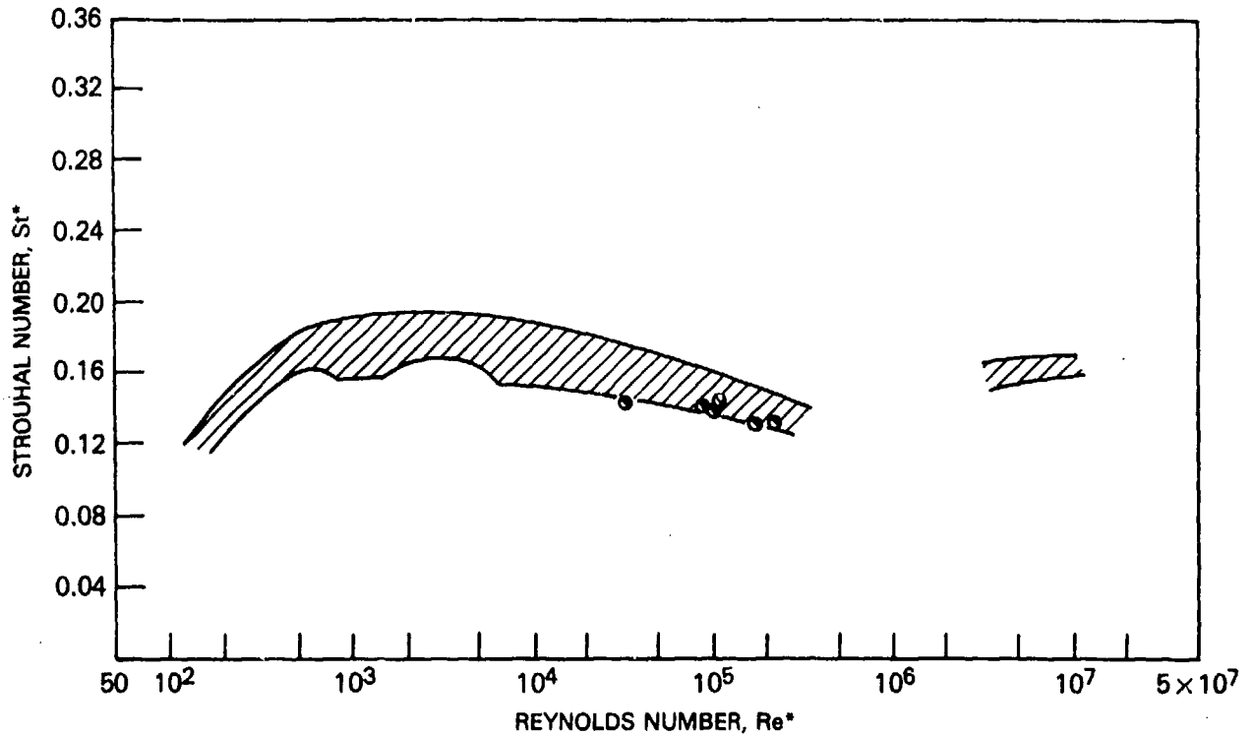

Figure 8. Universal Strouhal number St^* versus the Reynolds number Re^*. Shaded region (assorted stationary and vibrating bodies and flow conditions) from Griffin (19); data points, ●, from Peltzer and Rooney (23).

shaded region (19) all were measured in uniform flow over a host of stationary and vibrating two-dimensional bluff body cross-sections. It has been pointed out to the author (A. A. Szewczyk, private communication, 1981) that the universal Strouhal number—Reynolds number relationship is not valid when there are appreciable three-dimensional or secondary flow effects in the wake due to the shear flow past the cylinder. Agreement similar to that shown in Fig. 8 is not obtained when the flow in the wake is highly three-dimensional as in the experiments of Woo, Peterka and Cermak (22), for example. In their experiments appreciable secondary flow effects were evident in and downstream of the vortex formation region along the cable.

Elsner (24) has investigated the wake flow behind and the pressure distribution on a rectangular cylinder ($L/D = 7$) in a linear shear flow ($\bar{\beta} = 0.08$ to 0.09). The experiments were conducted in a low turbulence flow ($v'/V \sim 0.5$ percent) at Reynolds numbers from $Re_M = 10^4$ to 8×10^4. Pressure measurements around the model provided base pressure and drag coefficients. Measurements also were

made of the average drag coefficient using a force balance. Also measured with a hot wire anemometer were the wake width D', the local vortex shedding frequency f_s, and the vortex formation region length.

The findings from the experiments indicated that no universal Strouhal number St^* existed for the highly sheared flow since St^* varied continuously along the span of the model. However, the average value of St^* taken over the length of the cylinder was in good agreement with the data plotted in Fig. 8 over the comparable range of Reynolds numbers, $Re^* = 5 \times 10^4$ to 2×10^5.

In the shear flow the vortex shedding was organized into a cellular structure, with at least two distinct cells at all Reynolds numbers. There was evidence of additional cells developing at the higher Reynolds numbers. A clear jump in shedding frequency or Strouhal number was observed for this case of a small aspect ratio cylinder ($L/D = 7$). It was concluded by Elsner (24), from a study of his and previous investigations, that the length of a vortex shedding cell or filament was limited physically to about 5 diameters. The idea of a limiting length for the cells is supported by the results of Peltzer and Rooney (20, 23).

Recently a study was undertaken by Peltzer (25) to examine the flow about a flexible, helically wound marine cable of high aspect ratio ($L/D = 107$) that vibrated in a linear shear flow of steepness parameter $\bar{\beta} = 0.0053$. The Reynolds numbers of the experiments extended over the range $1.8 \times 10^3 \leqslant Re_M \leqslant 4 \times 10^4$. A strong cellular vortex shedding pattern was observed in the wake of the cable even at this relatively low shear level. Different distributions of spherical bluff bodies were added to the cable to simulate a marine cable with attached discrete masses. The attached bodies significantly altered the spanwise shedding pattern. A maximum separation distance of $\Delta\bar{z} = 20$ diameters was observed that forced the vortex shedding into discrete cells of constant frequency between the spheres. The presence of the spheres along the vibrating cable measurably increased the spanwise extent of the locked-on region, with the amount of increase being dependent upon the spacing between and number of the spheres.

Kiya, Tamura and Arie (26) studied the problem of vortex shedding from a circular cylinder when the axis of the cylinder was normal to the plane of the uniform, i.e., linear shear. The shear parameter varied from $\bar{\beta} = 0$ to 0.25 at Reynolds numbers from $Re = 35$ to 1500. The Strouhal number St_M versus Reynolds number variation for the condition $\bar{\beta} = 0.05$ is plotted in Fig. 9. The shear flow results are superimposed over corresponding uniform flow measurements by Kiya et al. and by Roshko (30). It is evident that a shear parameter of $\bar{\beta} = 0.05$ has little or no effect on the vortex shedding frequency for the shear flow/cylinder configuration studied by Kiya, Tamura and Arie.

When the shear parameter was increased to $\bar{\beta} = 0.2$ the Strouhal number St_M was increased substantially relative to the uniform flow case as shown in Fig. 10. There also is considerable scatter among the data for St_M at any given Reynolds number. It was concluded generally by Kiya, Tamura and Arie (26) that shear in the incident flow profile had little or no effect for $\bar{\beta} < 0.1$.

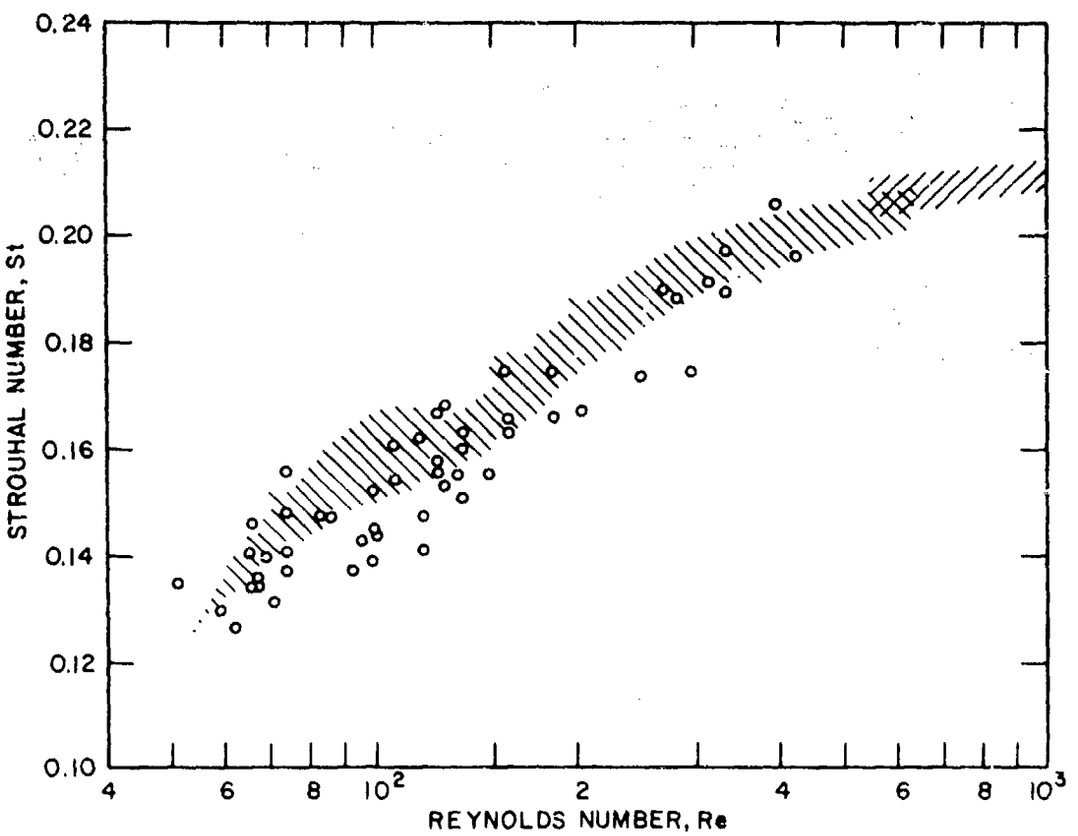

Figure 9 Strouhal number versus Reynolds number for shear flow, $\bar{\beta} = 0.05$. ○, Kiya, Tamura and Arie (26); ⧅, Kiya, Tamura and Arie (26), uniform flow; ⊠, Roshko's (1954) data for uniform flow in the range $Re > 550$. Reprinted with permission of the Cambridge University Press.

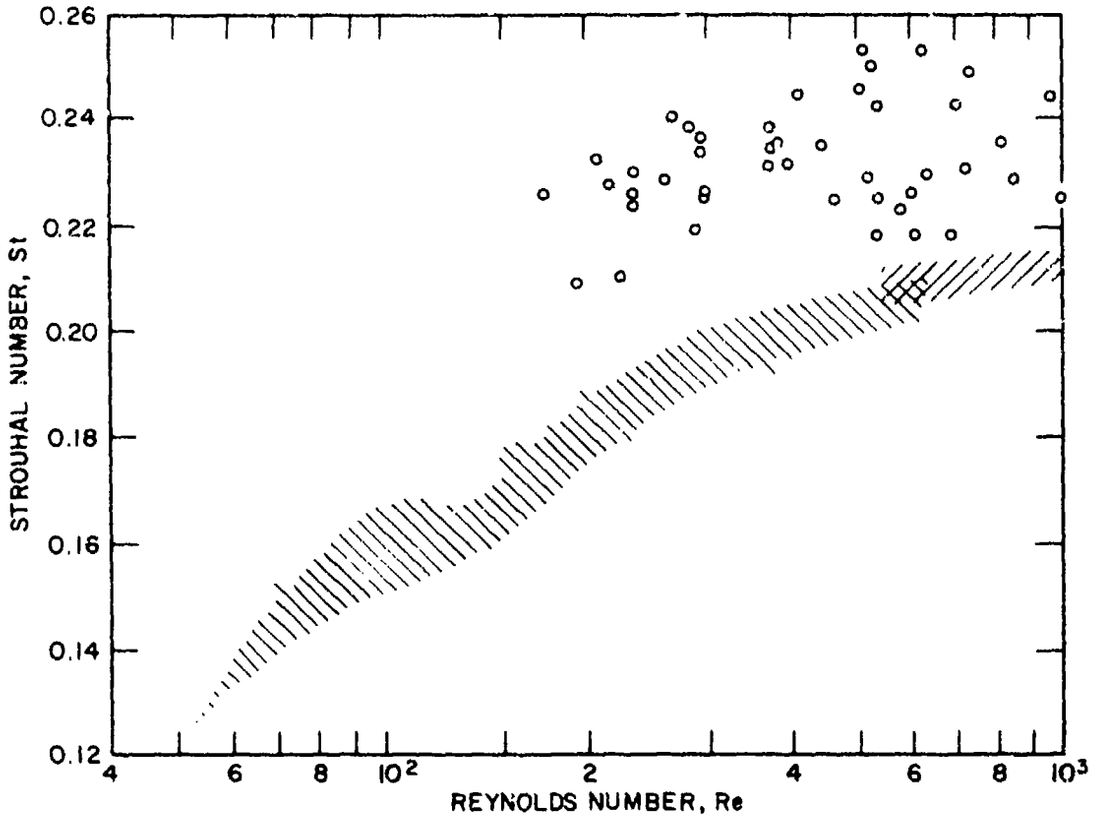

Figure 10. Strouhal number versus Reynolds number for shear flow. $K = 0.20$. Symbols as in Figure 9. Reprinted with permission of the Cambridge University Press.

4. THE EFFECTS OF BODY OSCILLATIONS

The combined effects of velocity gradients and body oscillations are difficult to quantify on the basis of available evidence. However, the relatively sparse information that is available suggests that model and full-scale cylindrical structures will vibrate at large displacement amplitudes in both air and water even in the presence of nonuniform flow effects if the reduced damping is sufficiently small and the critical reduced velocity is exceeded (see Figs. 11 and 14 and Appendix I). Some detailed experiments reported just recently by Kwok and Melbourne (31) give strong evidence that a flexible bluff structure with a circular cross-section will vibrate resonantly at large displacement amplitudes when a turbulent boundary layer type of shear flow is incident upon the cylinder. Kwok and Melbourne measured large tip displacements of up to $\bar{Y} = 0.3\ D$ for reduced dampings in the range $k_s = 2$ to 12 ($\zeta_s/\mu \sim 0.5$ to 3). A typical example of their findings is given in Fig. 11.

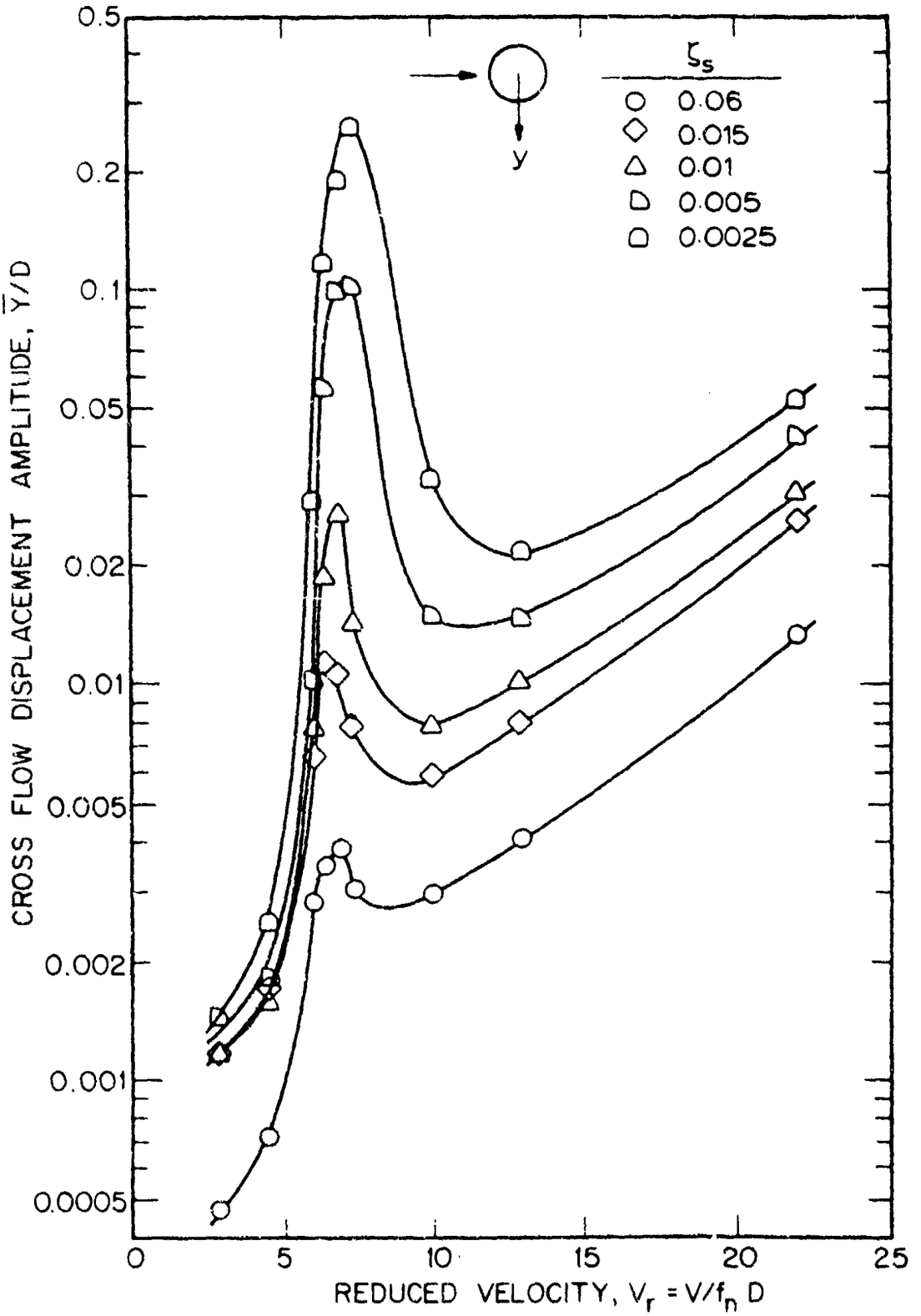

Figure 11. Peak cross flow displacement response $\bar{Y}/D$ (standard deviation of $\bar{Y}$) plotted against reduce velocity $V_r = V/f_n D$ for a model circular cylinder in a turbulent boundary layer, from Kwok and Melbourne (31). The structural damping ratio ζ_s of the rigid pivoted model was varied as shown on the figure. The characteristic flow velocity V was measured at the tip of the cylinder, of aspect ratio $L/D = 9$. The figure was provided by Dr. K.C.S. Kwok, University of Sydney, Australia.

Stansby (15) investigated the phenomenon of lock-on for the cross flow vibrations of circular cylinders in a linear shear flow and has compared the results to comparable experiments in uniform flow. From these experiments Stansby developed empirical equations to predict the bounds for lock-on in a shear flow, based upon the assumption of universal similarity of the flow in the wakes of bluff bodies (18,19). The boundaries of the cross flow lock-on regime that were measured by Stansby are shown in Fig. 12. However, these results are limited to cylinders with small length/diameter ratios (L/D = 8 to 16), relatively low Reynolds number (Re = 3000 to 10,000), and small displacement amplitudes ($\bar{Y}/D < 0.2$). These results are considered in further detail in the next section of this report.

The measured Strouhal numbers for stationary and vibrating circular cylinders in a shear flow are compared in Fig. 13. The measurements were reported by Stansby (15) for $Re_M \approx 4000$ and $\bar{\beta} = 0.025$. The stationary cylinder wake is dominated by two end cells with an irregular type of vortex

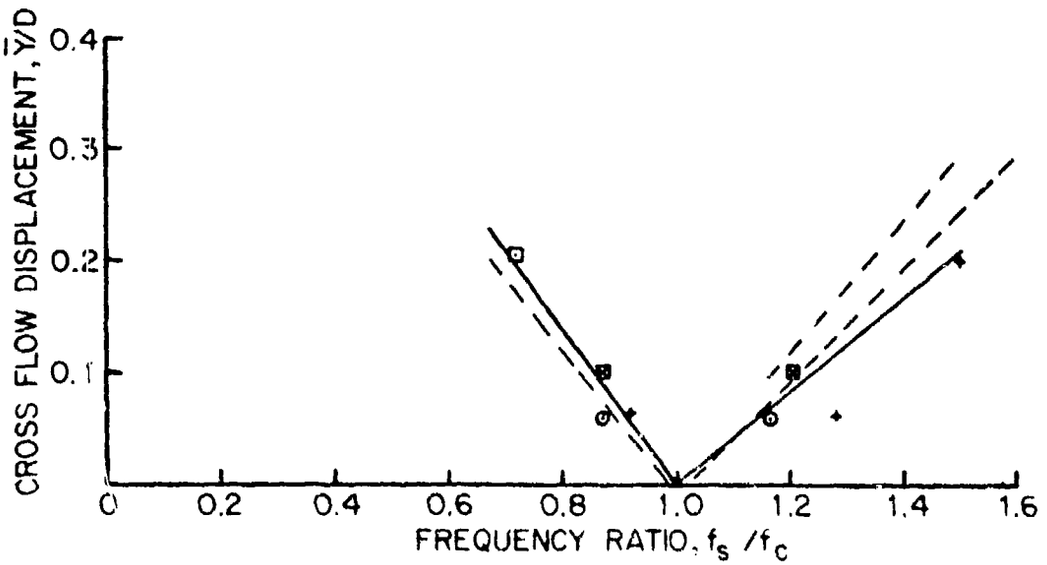

Figure 12. Boundaries of the cross flow lock-on regime in a shear flow, denoted by the displacement amplitude $\bar{Y}/D$ on the vertical scale plotted against the ratio f_s/f_c of the Strouhal and vibration frequencies, from Stansby (15). Reprinted by permission of the Cambridge University Press. Legend for data points

$St_M = fD/U_M = 0.168$, $L/D = 9$, $Re_M = 9100$.

○ $St_M = 0.198$

\+ $St_M = 0.155$ $L/D = 16$, $Re_M = 5700$.

$St_M = 0.134$

---- Uniform flow (15)

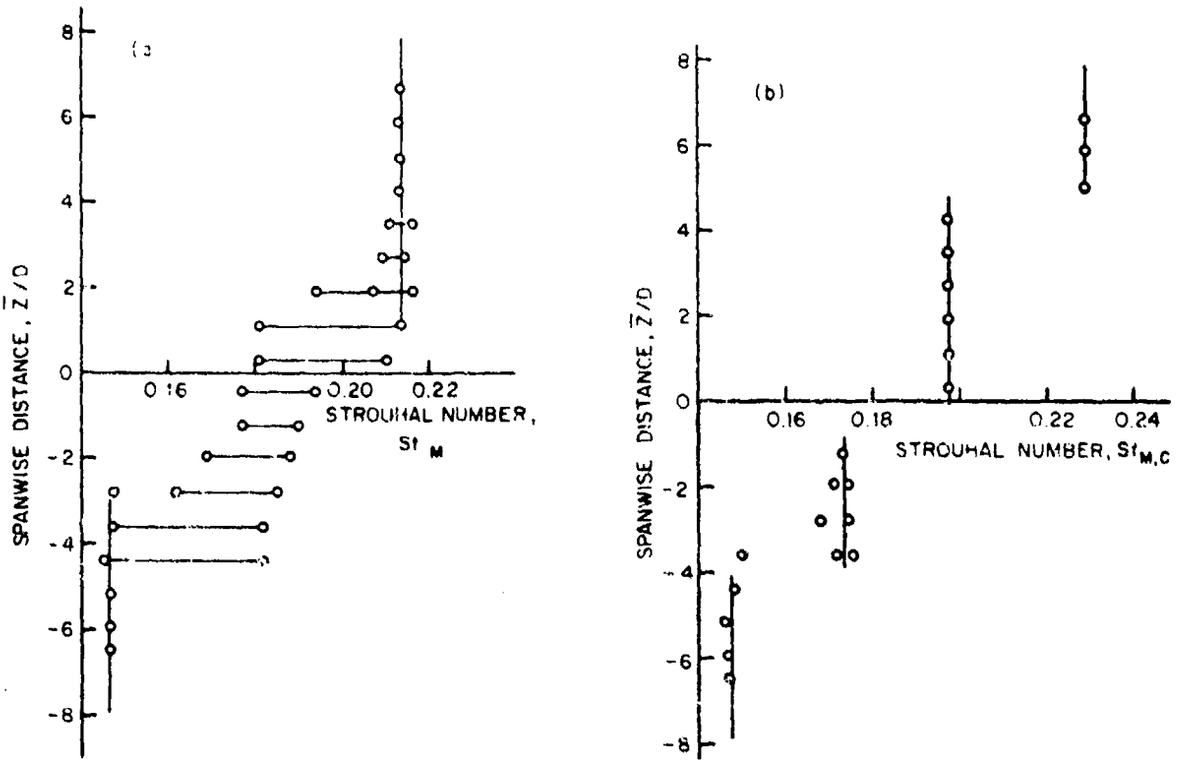

(a) Stationary cylinder. Reynolds number $Re_M \approx 4000$, shear flow steepness parameter $\bar{\beta} = 0.025$, cylinder aspect ratio $L/D = 16$.

(b) Vibrating cylinder. Same conditions as Figure 13(a) except that the forced Strouhal number of the cross flow oscillation is $St_{M,c} = 0.198$, displacement amplitude $\bar{Y}/D = 0.06$.

Figure 13. Strouhal number St_M plotted against the spanwise distance along stationary and vibrating cylinders; from Stansby (15). Reprinted by permission of the Cambridge University Press.

shedding between these cells. This irregular region is characterized by a wide frequency spectrum which represents a range of cell shedding conditions, and the Strouhal number ranges in Fig. 9(a) define the ranges of possible constant-frequency vortex shedding cell formation. When the same cylinder was oscillated at a forced Strouhal number of $St_{M,c} = 0.198$, the vortex shedding over the center portion of the cylinder was dominated by a single cell from $\bar{z}/D = -1$ to $+4$ that was locked to the vibration frequency as shown in Fig. 13(b). The three unforced cells that are distributed along the cylinder show considerably more regularity in shedding frequency than do the corresponding cells on the stationary cylinder.

A recent paper and a report by Fischer, Jones and King (32,33) describe some problems that were anticipated during the installation of foundation piles for the Shell Oil production platform in the Cognac field of the Gulf of Mexico. The problems largely stemmed from the predicted vortex-excited

oscillations of the piles while they were being lowered from a derrick barge into sleeves in the platform base and while the inserted piles were being hammered into the sea bed. Maximum tip displacement amplitudes (cross flow) of 3.2 to 3.8 m (10.5 to 12.5 ft) from equilibrium were predicted for currents as low as 0.6 m/s (0.31 kt) at the platform site. These large-scale motions were expected to create difficulties while "stabbing" the piles into the sleeves, and they could also increase the risk of buckling and fatigue failures during the pile driving operations. Experiments were conducted with model piles in three laboratories, for both the pile lowering and the pile driving operations. Uniform and nonuniform (shear) flows were modelled in the experiments. For the small-scale experiments reported by Fischer, Jones and King (32,33) the shear parameter was $\bar{\beta} = 0.015$ while at the actual Cognac site $\bar{\beta} = 0.01$ at depths between 100 m (330 ft) and 250 m (820 ft).

The results from some typical model-scale experiments are plotted in Fig. 14. The tests were conducted with a 1:168 scale model of the large marine piles of diameter $D = 2.1$ m (6.9 ft). Both the full-scale and the model piles had specific gravities of 1.5. It is clear from the results in Fig. 14 that a shear flow with $\bar{\beta} = 0.01$ to 0.015 had virtually no effect on the vortex-excited displacement amplitudes in the cross flow direction. The data plotted in the figure correspond to a free-cantilever flexible beam with no tip mass at the free end. This configuration matched closely the "stabbed" pile before an underwater hammer was attached for driving it into the sea bed. The structural damping of the PVC model in Fig. 14 was $\zeta_s = 0.063$ and for a similar stainless steel model the damping was $\zeta_s \approx 0.015$; the two flexible cylinders experienced tip displacement amplitudes of $2\bar{Y} = 3\ D$ and $4\ D$, respectively. These damping and displacement amplitude values are in the range of mass and damping parameters where hydrodynamic effects are dominant (34); see Fig. 24.

It was concluded from a study of the static and dynamic stress levels within the Cognac piles during driving that the large cross flow displacement amplitudes (of the level shown in Fig. 14) would triple the stresses from a corresponding stationary 130 m (426 ft) long pile (30). The apparent steady drag coefficient on the oscillating pile was $C_D = 2.12$; this is an amplification of 230 percent from the drag coefficient $C_{DO} = 0.93$ when the pile was restrained. A fatigue life of four days was predicted for

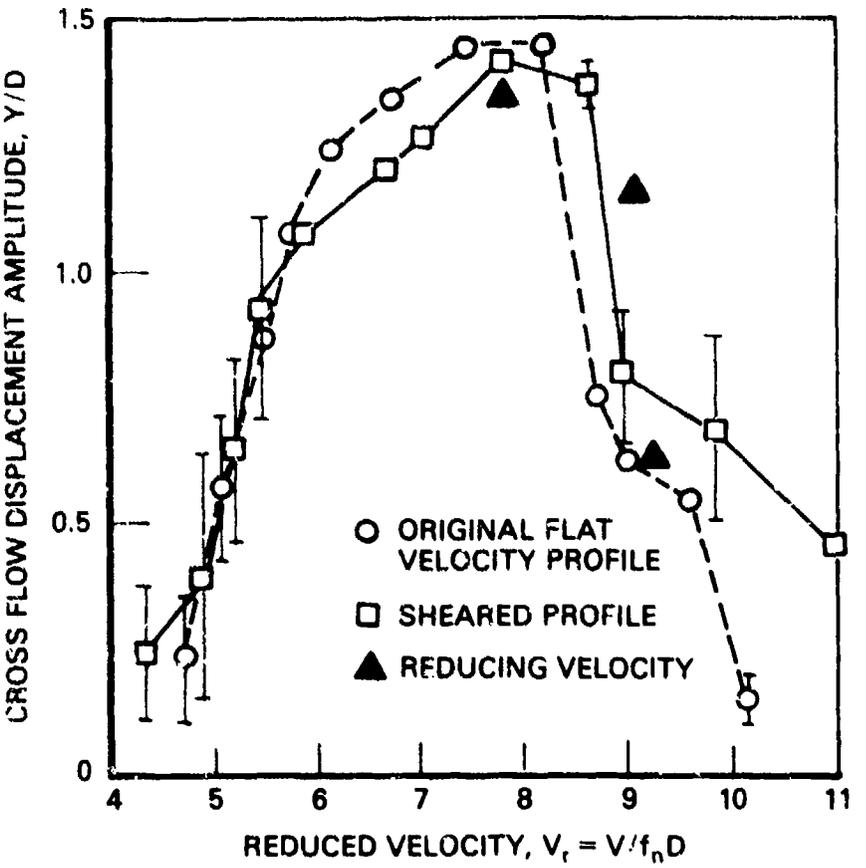

Figure 14. Measured peak cross flow displacement amplitude $\bar{Y}/D$ plotted as a function of the reduced velocity V_r. A slender, fully submerged and cantilevered circular cylinder was employed as the model (L/D = 52, D = 12.7 mm (0.5 in)) for experiments conducted in uniform ($\bar{\beta}$ = 0) and shear ($\bar{\beta}$ = 0.01 to 0.015) flows of water. The cylinder was a 1:168 scale model of a full-scale marine pile with the same specific gravity (SG = 1.5), from experiments reported by Fischer, Jones and King (32) and King (33). In the case of the shear flow V is the maximum value in the nonuniform incident velocity profile. The figure was provided by Dr. Warren Jones of the Shell Development Company.

a stabbed pile (without a hammer attached) when it was exposed to a current of 0.46 m/sec (0.9 kt) in magnitude. Additional details and assumptions pertaining to the study are discussed in references 32 and 33.

Experiments with flexibly-mounted cylinders in uniform and shear flows were conducted in a wind tunnel by Howell and Novak (35). When the complications of various types of turbulence and boundary layer-type shear profiles were added to the case of a low-turbulence uniform flow, Howell and

Novak found that the displacement response of the cylinder was largely independent of the flow characteristics *if the structural damping was sufficiently small to cause lock-on*. Examples of four types of incident wind flow and their effect on the displacement amplitude response of a circular cylinder are shown in Fig. 15.

As the damping ratio was increased from the value ($\zeta_s = 0.01$) corresponding to the results in Fig. 15, the displacement response of the flexibly-mounted cylinders became susceptible to the characteristics of the incident flow to the cylinder. The measured displacement amplitudes compare very well with those found by other investigators, and full lock-on was observed for this cylinder with $\zeta_s = 0.01$ and $\bar{Y}/D \approx 0.25$. Fig. 16 shows a flexibly mounted circular cylinder that is placed in a deep turbulent boundary layer. The large cross flow displacement amplitude of the cylinder is plainly visible in the photograph. These findings demonstrate further that flexible cylindrical structures with small reduced damping ζ_s/μ will be susceptible to resonant vortex-excited oscillations even if the incident flow is highly nonuniform.

Kwok and Melbourne (31) also measured the cross flow response of a flexibly-mounted square cylinder. A similar variation of the displacement amplitude with structural damping as had been observed with a circular cylinder was found again for the square cylinder in the boundary layer type of incident shear flow. Other studies with square and rectangular cross-section models are discussed in the Proceedings of the Fifth International Conference on Wind Engineering, held in 1979 (36) and the Proceedings of the Fourth International Conference on Wind Effects on Buildings and Structures, held in 1975 (37).

Woo, Peterka and Cermak (22) have conducted experiments to study the effects of shear on vortex shedding from flexible cables. Experiments were conducted at Reynolds numbers from $Re = 700$ to 1700 with cables that were forced to oscillate in shear flows with steepness parameters from $\bar{\beta} = 0$ to 0.036. Some examples of the results that they obtained are given in Figs. 17 and 18. The frequency spectra from the wake of a stationary cable in a shear flow in Fig. 17 show no cell structure, and the frequency of the vortex shedding varies linearly over the entire span ($L = 40\ D$) of the cable. When

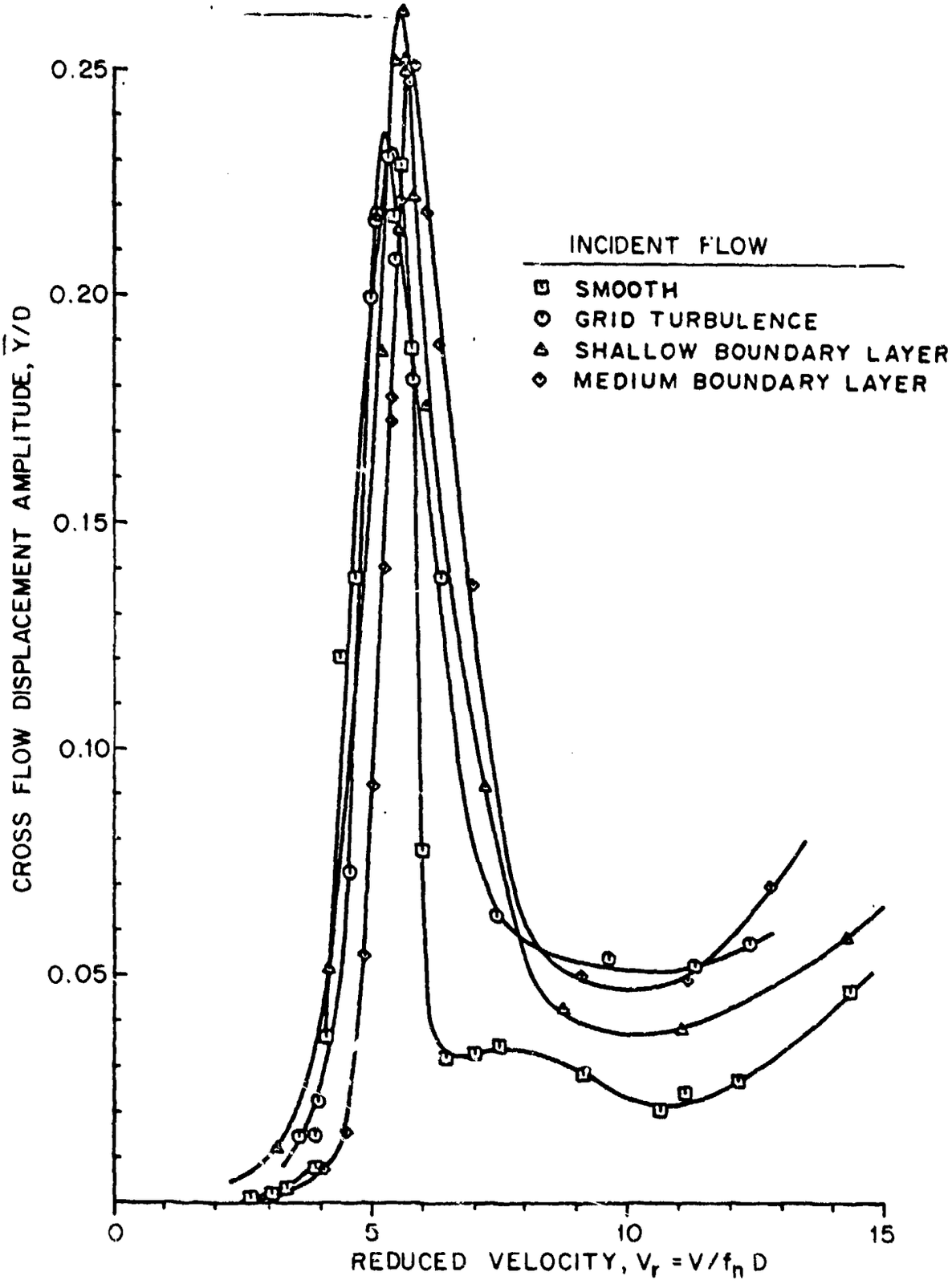

Figure 15. Peak cross flow displacement amplitude $\bar{Y}/D$ (root-mean-square of $\bar{Y}$) plotted against reduced velocity V_r for a flexibly-mounted circular cylinder in uniform and sheared incident flows; from Howell and Novak (35). Structural damping ratio $\zeta_s = 0.01$, aspect ratio $L/D = 10$. The various types of incident wind flows are given by the legend. The figure was provided by Dr. John F. Howell, VIPAC Ltd., South Yarra, Vic., Australia.

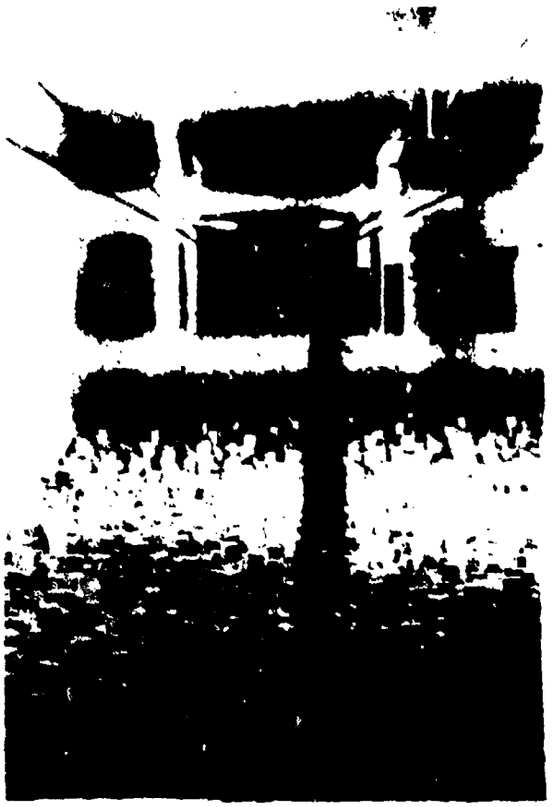

Figure 16. Cross flow oscillation of a flexibly-mounted circular cylinder in a deep boundary layer type of incident shear flow (34). The photograph was provided by Dr. John F. Howell, VIPAC Ltd., South Yarra, Vic., Australia.

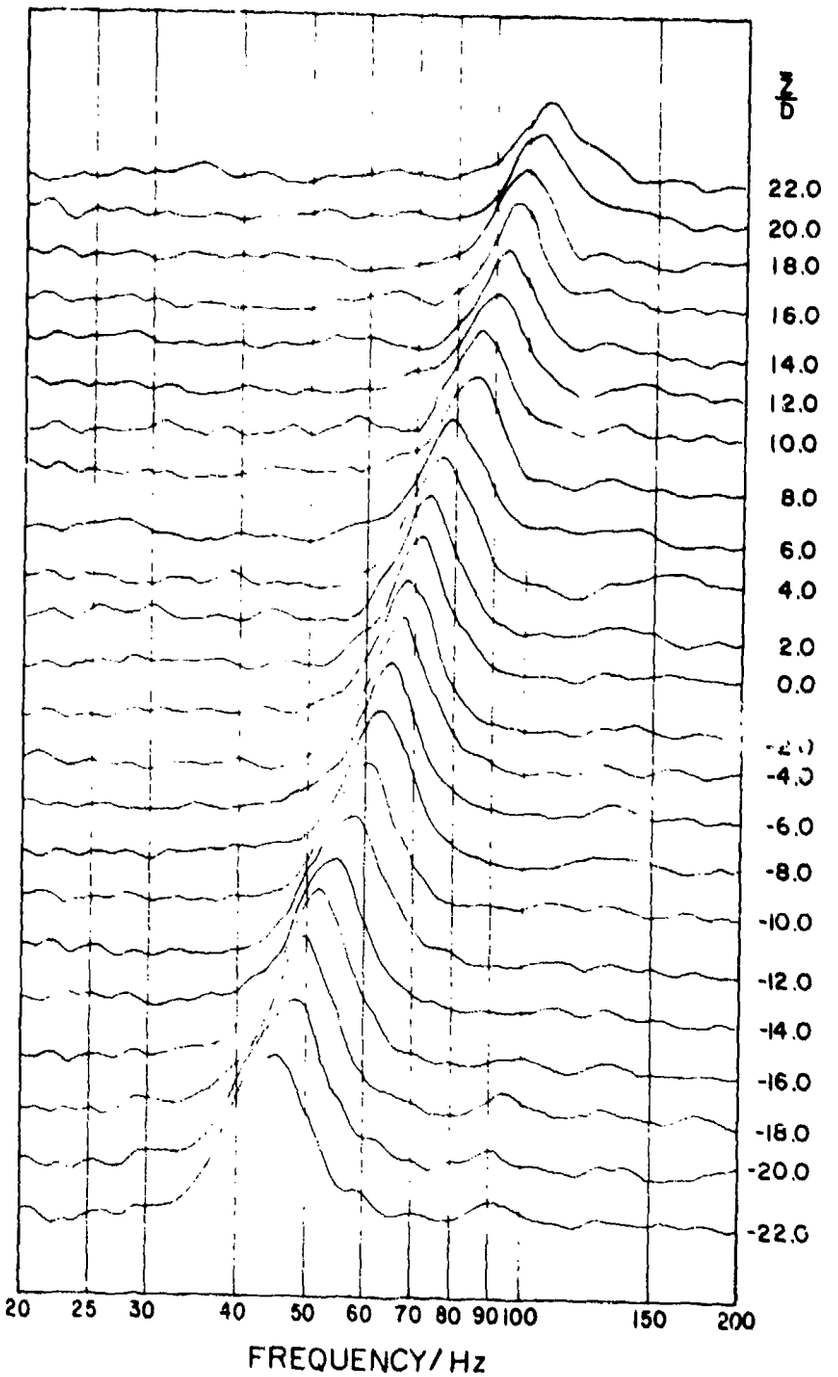

Figure 17. Frequency spectra at various positions for an oscillating cylinder with $D = 0.25$ in.; $L/D = 40$; $a/D = 0.0$; $Re_m = 725$ and $\beta_m = 0.016$; from Woo, Peterka and Cermak (22).

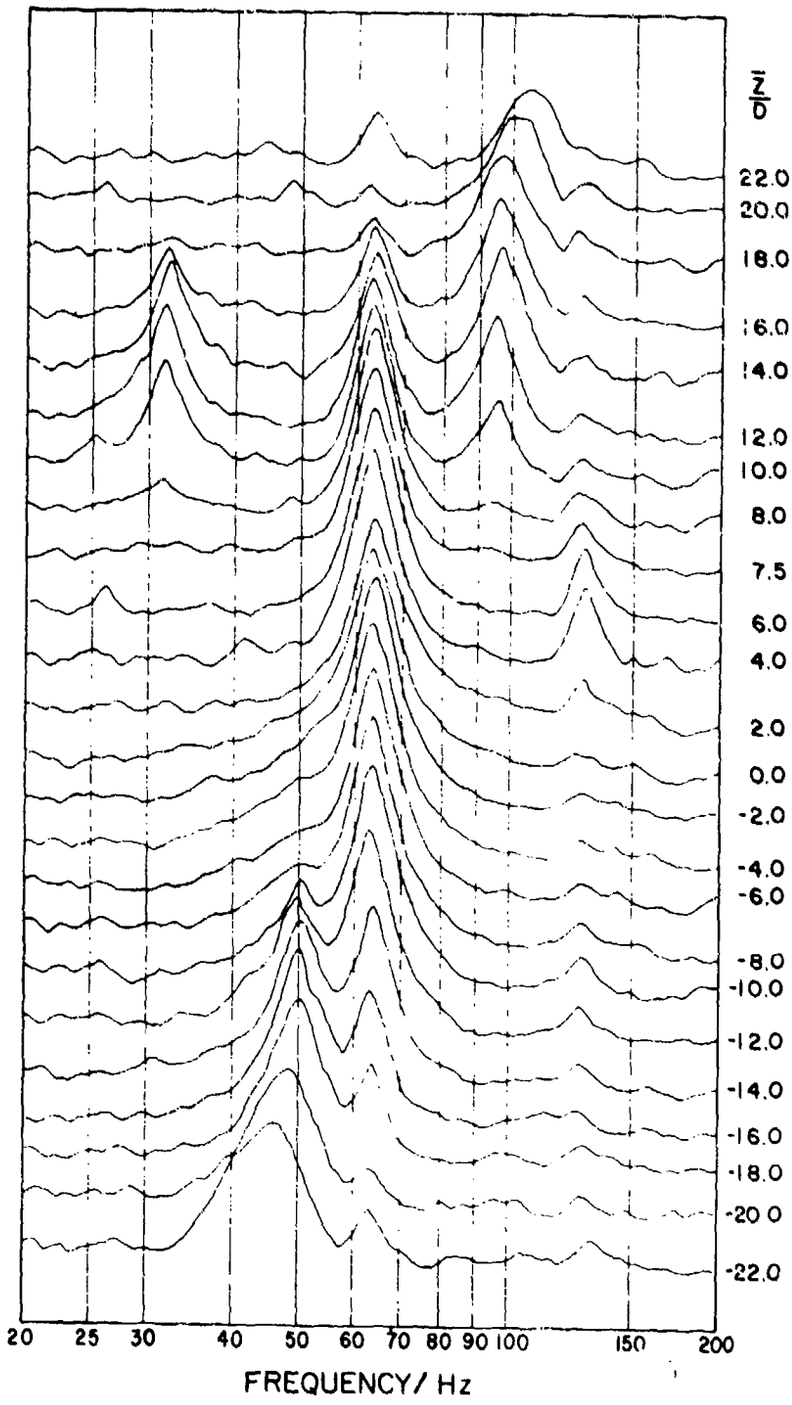

Figure 18. Frequency spectra at various positions for an oscillating cylinder with $D = 0.25$ in.; $L/D = 40$; $a/D = 0.0$; $Re_m = 735$ and $\beta_m = 0.016$; from Woo, Peterka and Cermak (22).

the cable was vibrated normally to the flow at about 88% of the center-span shedding frequency and at about a half-diameter (peak-to-peak), the vortex shedding frequency spectra were altered as shown in Fig. 18. There is a lock-on region at a single (vibration) frequency f from about $z = 8\ D$ to $z = -4\ D$, or $\Delta\bar{z} \simeq 12\ D$. For $z < -4\ D$ clear peaks are present in the frequency spectra of the local shedding frequency and the vibration freq iency (no lock-on). For $z > 8\ D$ again the spectra contain clear peaks at both the local vortex shedding frequency and the vibration frequency. Many of the spectra contain a distinct frequency contribution at the second harmonic $2f$ and some ($z = 8.5\ D$ to $16\ D$) contain an apparent contribution at the difference $(f_{s,z} - f)$ between the local shedding frequency $f_{s,z}$ and the vibration frequency f.

The local bounds for the region of the locking on are given below as obtained by Woo, Peterka and Cermak. In terms of least-squares fitted curves the results are

$$\left(\frac{St_{SM}}{St_{CM}}\right)_{-} = 1.03 + 0.41\ (2\bar{Y}/D)^{.452} \tag{2}$$

and

$$\left(\frac{St_{SM}}{St_{CM}}\right)_{+} = 0.96 - 0.88\ (2\bar{Y}/D) + 3.88\ (2\bar{Y}/D)^2 - 3.7(2\bar{Y}/D)^3. \tag{3}$$

Equation (2) corresponds to the boundary region at the high velocity end of locking-on and Eq. (3) corresponds to the low velocity boundary region. In general it was found that $St_{SM}/St_{CM} \geqslant 0.9$ for the cable oscillation to lock on to the vortex shedding in the shear flow. In addition, the local values of the Strouhal number along the stationary cable were found to be essentially constant at $St = f_s D/V = 0.22$ for the experiments just described (22).

Experiments were conducted by Peltzer (25) to study the effects of shear on vortex shedding from stationary and vibrating marine cables. In some of the experiments, a distribution of spheres was attached to the cable to simulate the effect of attached bodies such as sensor housings and buoyancy

elements. The cable of 11.4 mm (.045 in) diameter had a length to diameter ratio of $L/D = 107$, which resulted in a shear flow steepness parameter $\bar{\beta} = 0.0053$ over the Reynolds number range $Re = 1.8 \times 10^3$ to 4×10^4.

The spanwise Strouhal number variation along the stationary cable in the shear flow is shown in Fig. 19. There are ten cells of constant Strouhal number along the cable span. The average length of the cells is eleven cable diameters and the change in the Strouhal number from cell to cell is $\Delta St_M = 0.0086$. There is a total change in the Strouhal number of $\Delta St_M = 0.067$ across the span from $-48 \leqslant \bar{z}/D \leqslant 48$. The clarity of the cellular structure is due to a careful optimization of the location of the hot-wire probe that was used to sense the frequency of vortex shedding from the cable (25).

The cable was oscillated in its first mode with an antinodal displacement amplitude of 2 $\bar{Y} = 0.29D$ and at a reduced velocity of $V_r = 5.6$. The vortex shedding pattern in Fig. 19 was changed by the oscillations as shown in Fig. 20. The vortex shedding was locked-on to the cable vibration over

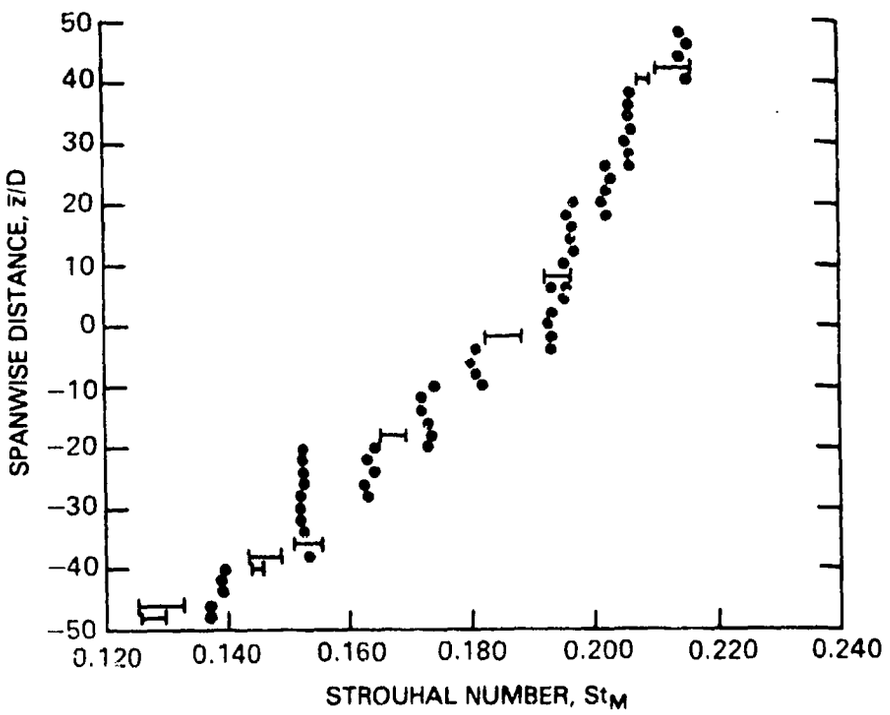

Figure 19. Strouhal number St_M plotted against spanwise distance along a stationary flexible cable in a linear shear flow; from Peltzer (25). Reynolds number $Re_M = 2.96 \times 10^3$, shear flow steepness parameter $\bar{\beta} = 0.0053$.

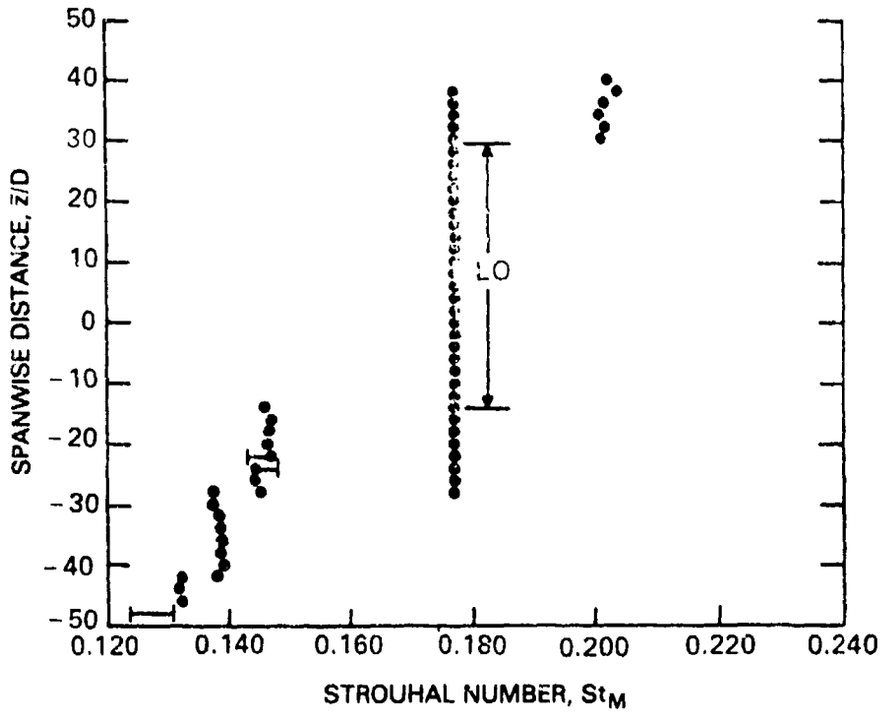

Figure 20. Strouhal number St_M plotted against spanwise distance along a vibrating flexible cable in a linear shear flow; from Peltzer (25). Reynolds number $Re_M = 2.96 \times 10^3$, shear flow steepness parameter $\bar{\beta} = 0.0053$, reduced velocity $V_r = 5.6$, displacement amplitude (first mode) $2\bar{Y} = 0.29D$.

the central portion of the cable span from $-14 \leqslant \bar{z}/D \leqslant 30$, so that the locked-on cell was 44 diameters long. The remainder of the vortex shedding pattern not influenced by end effects was stabilized as well. Two cells were increased in length to fourteen diameters each and no fluctuations in the cell boundaries were observed. The change in the Strouhal number across the span was increased to $\Delta St_m = 0.078$ (25).

One of the objectives of these experiments was to investigate the effects of attached bluff bodies on the vortex shedding. The vortex shedding pattern along the cable with five spheres (ping pong balls) attached is shown in Fig. 21. The flow conditions were the same as in Figs. 19 and 20, except that the antinodal displacement amplitude of the cable was $2\bar{Y} = 0.23D$.

Several points concerning the vortex shedding from the cable-sphere system are notable. The three central spheres ($\bar{z}/D = -20, 0, 20$) locked-on to a submultiple (one half) of the cable vibration frequency. The lock-on region of the cable strumming in Fig. 21 extended from $-24 \leqslant \bar{z}/D \leqslant 29$, or over 53 diameters. This is a significant increase from the comparable bare cable experiments. For

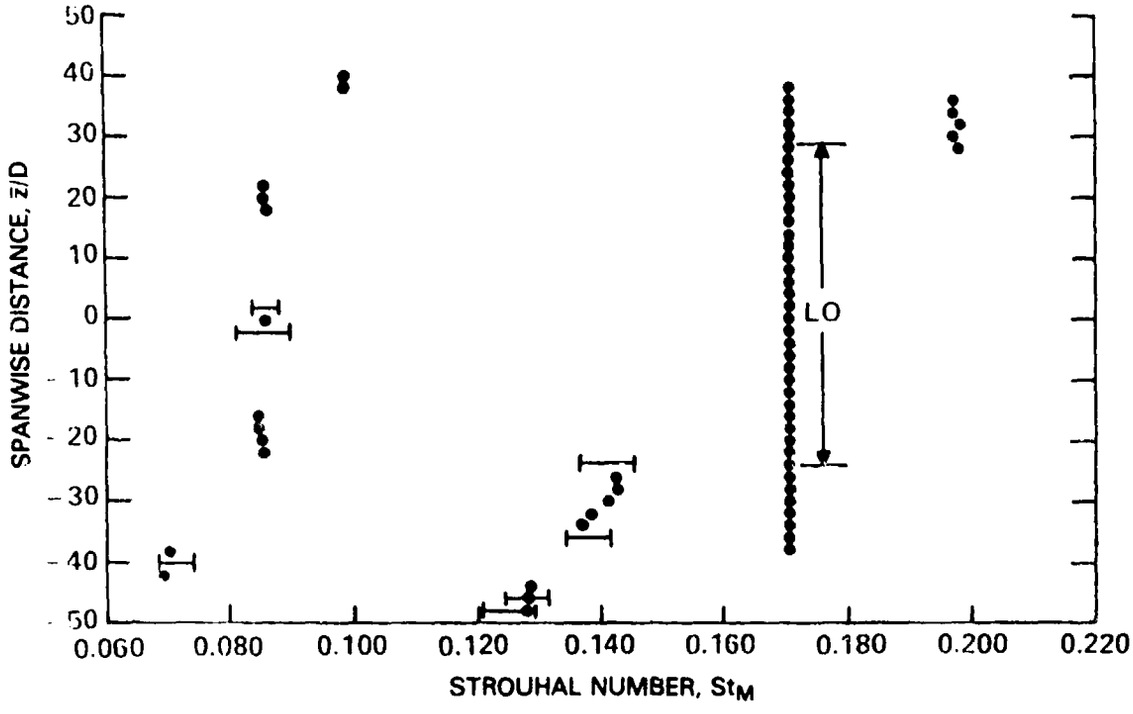

Figure 21. Strouhal number St_M plotted against spanwise distance along a vibrating flexible cable with five attached spheres in a linear shear flow; from Peltzer (25). Conditions as in Figure 20 except that $2\bar{Y} = 0.23D$.

example, when $2\ \bar{Y} = 0.29D$ for the bare cable the lock-on region extended over 44 diameters, and when $2\ \bar{Y} = 0.23D$ the lock-on region extended over 34 diameters. When three spheres ($\bar{z}/D = -28$, 0, +28) were attached to the cable, with $2\ \bar{Y}/D = 0.235$, the lock-on region extended over 61 cable diameters. It is clear that the addition of attached bodies along the cable is not likely to deter the resonant cable strumming vibrations even in a shear flow.

Similar results have been reported by Vandiver and Griffin (38). In 1981 a program of field experiments was conducted to investigate the effects of attached masses on cable strumming. The cable was 23 m (75 ft) long and 32 mm (1.25 in) in diameter and was placed in a spatially uniform tidal current environment. It was observed that arrays of attached cylindrical masses (up to seven) did not deter the cable strumming. Even the cylindrical masses vibrated at displacement amplitudes up to $\bar{Y} = \pm\ 0.3D$ (RMS). The drag coefficients on the cable with and without attached masses consistently were in the range $C_D = 2.4$ to 3.2 over time periods up to two and one half hours. This is a considerable increase over the drag coefficients ($C_D = 1.2$ to 1.4) that would be expected if the cable was restrained from oscillating.

Peltzer (25) observed other significant features relating to cable strumming in a shear flow. A maximum separation distance of twenty cable diameters between the spheres was observed that would force the vortex shedding into cells of constant frequency when the cable was stationary. The cellular structure along the cable with spheres attached was forced into a pattern that was appreciably different from the bare cable in the shear flow when the spacing between the spheres was twenty diameters or less.

5. A METHOD FOR ESTIMATING THE BOUNDS OF FREQUENCY LOCK-ON IN A SHEAR FLOW

It is possible, based upon the recent work of Stansby (15), Griffin (18,19), Woo, Peterka and Cermak (22), and Peltzer (25) to predict the spanwise extent over which the vortex shedding is locked onto the vibrations of a flexible circular cylinder or cable in a shear flow. Many of the characteristics of flow past a rigid cylinder can be extended to the analogous case of a slender bluff body such as a cable or other flexible bluff structure, as recent findings have shown (39,40). The vibrating cable experiments of Woo, Peterka and Cermak provide additional data upon which to base a proposed method of prediction for the extent of lock-on in a shear flow.

The method to be described is dependent upon several assumptions:

(i) The structure or cable has a high aspect ratio, i.e., $L/D > 20$;

(ii) The *local* Strouhal number is constant or varies only slightly;

(iii) The velocity profile of the shear is linear or nearly so;

(iv) The shear parameter $\bar{\beta}$ is limited to moderate values, i.e., $\bar{\beta} < 0.03$.

The first assumption is necessary because the effects of end boundaries and the vortex shedding cells that are common at the ends of a cylinder should be negligible. Only cylinders with $L/D >> 20$ have regions of vortex shedding that are free of end cell effects. The model to be described below is based

upon the supposition that the *local* Strouhal number is constant; this necessitates the second assumption. Virtually all of the available results for vortex shedding from bluff bodies in a shear flow have been obtained with linear incident velocity profiles. Thus any model derived from the existing data base, strictly speaking, will be limited in application to linear shear flows. Many practical flows in air and in water are limited to moderate values of the shear parameter, i.e., $\bar{\beta} \approx 0.01$ to 0.015 (31,32), so that limiting the model to the range $\bar{\beta} < 0.03$ will have no serious consequences in terms of practical application.

Stansby (15) proposed a model for predicting the extent of frequency lock-on in a shear flow. The model was based upon the results obtained from experiments with an oscillating rigid cylinder in a linear shear flow. The equation derived by Stansby for the extent, $\Delta\bar{z}$, of locking-on is

$$\frac{\Delta\bar{z}}{D} = \frac{4.0}{\bar{\beta}_M}\left|\frac{2\bar{Y}}{D}\right|\frac{St_M}{St}, \tag{4}$$

where $St_M = fD/V_M$ and St is the local Strouhal number ($St = f_sD/V$). The details of the derivation and the assumptions upon which it is based are given by Stansby (15). The primary assumption is the validity of a universal Strouhal number (18,19) for the cylinder in a shear flow. The results of Vickery, Peterka and Cermak (22) show that because of large secondary flow effects the concept of universal similarity may not be valid for a cylinder in a shear flow when such effects are present. Elsner (24) since has confirmed that the universal similarity hypothesis cannot be sustained at large values of the shear parameter ($\bar{\beta} = 0.08$ to 0.09). On the other hand, the experiments of Peltzer and Rooney (23) give universal Strouhal numbers for cylinders in a shear flow that are in reasonable agreement with the results summarized by Griffin (19) for a cylinder in a uniform flow. The latter experiments were conducted at relatively small values of the steepness parameter ($\bar{\beta} < 0.01$) so that secondary flow effects were small.

The equation proposed by Stansby is not valid in the case of a flexible cable or structure because the amplitude of oscillation is not constant along the span of the body. A more complete model is required that takes into account the shedding frequency variation, the changing spanwise distribution of

oscillation amplitude, and the shear velocity profile. Woo, Peterka and Cermak (22) and Peltzer (25) have provided a initial data base that takes all of these factors into account. The Reynolds numbers of their experiments are limited to values below 4×10^4, but the data provides the basis for a more general equation similar to the one given originally by Stansby.

The boundaries of the region of locking-on given by Eqs. (2) and (3) can be simplified for the purposes of the present approach. The results are plotted in Fig. 22. The data points there correspond to the conditions that are most representative of resonant, flow-induced oscillations. It is clear from the data shown that the frequency bounds for the lock-on in a shear flow are essentially constant for $2\bar{Y}/D > 0.2$. The coherence lengths of the vortex shedding along the cable in the shear flow, corresponding to the data plotted in Fig. 22 and those of Peltzer (25), are plotted in Fig. 23. It is clear that the coherence length of the vortex shedding has approximately an inverse relation to the shear parameter $\bar{\beta}$.

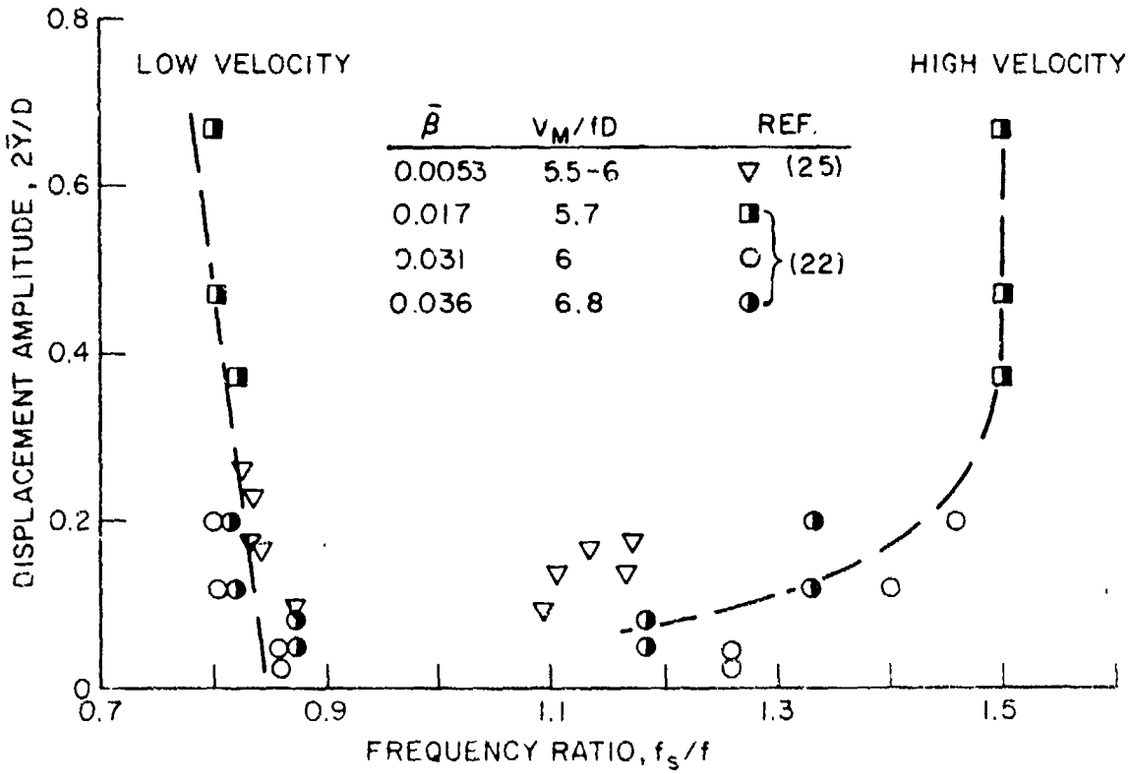

Figure 22. The local displacement amplitude and frequency boundaries for the lock-on between vortex shedding and cable vibrations in a shear flow, data from Woo, Peterka and Cermak (22); and Peltzer (25).

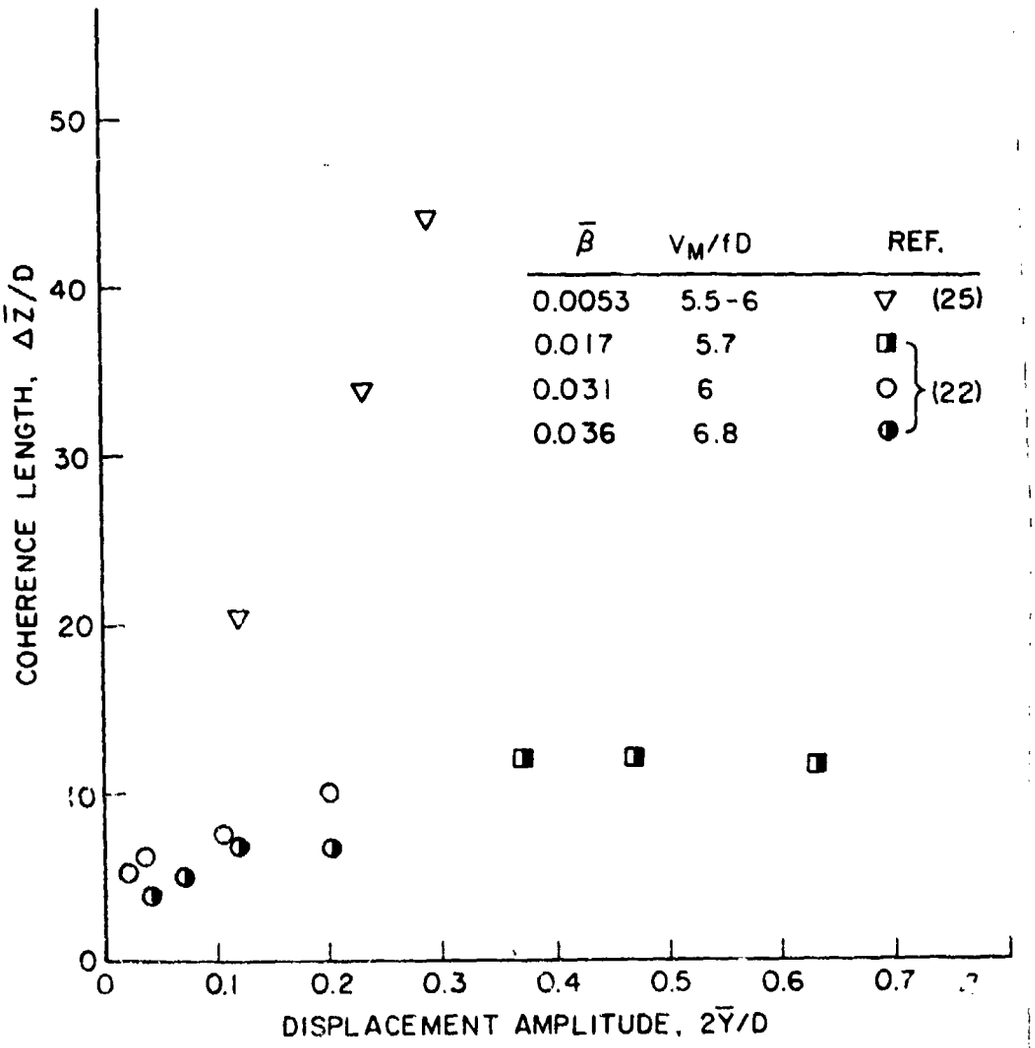

Figure 23. Coherence length $\Delta\bar{z}$ of the vortex shedding from a vibrating flexible cable in a shear flow; data from Woo, Peterka and Cermak (22); and Peltzer (25).

On the basis of these results an approach can be taken as follows. The local Strouhal number is

$$St = \frac{f_s D}{V}$$

or, equivalently

$$St_M = \frac{f_s D}{V_M} = St\left(\frac{V}{V_M}\right) = St\left(1 + \left|\frac{\bar{z}}{D}\right|\bar{\beta}\right). \tag{5}$$

At the high velocity end of the lock-on region,

$$St_M|_2 = St\left(1 + \frac{\bar{z}_2}{D}\,\bar{\beta}\right) \tag{6a}$$

and at the low velocity end

$$St_M|_1 = St\left|1 + \frac{\bar{z}_1}{D}\,\bar{\beta}\right| \tag{6b}$$

where local values of the displacement amplitude z_2 and z_1 are used. If the reduced velocity $V_{rM} = V_M/fD$ is introduced, then

$$V_{rM}^{-1}\left[\frac{f_s}{f}|_2 - \frac{f_s}{f}|_1\right] = St\,\bar{\beta}\left[\frac{\bar{z}}{D}|_2 - \frac{\bar{z}}{D}|_1\right] \tag{7}$$

is obtained when Eq. (6b) is subtracted from Eq. (6a). The vibration frequency f is constant and it should be noted again that the local Strouhal number St is assumed to be constant in this formulation. Simplifying the terminology,

$$V_{rM}^{-1}\,\Delta\left(\frac{f_s}{f}\right)_{2-1} = St\,\bar{\beta}\,\Delta\left(\frac{\bar{z}}{D}\right)_{2-1}. \tag{8}$$

The frequency difference $\Delta(f_s/f)_{2-1}$ can be approximated by the results in Fig. 22; for $2\bar{Y}/D > 0.2$, $\Delta(f_s/f)_{2-1} \simeq 0.7$. A more complicated approach involving the simultaneous solution of these equations was proposed by Woo, Peterka and Cermak (22), based upon Eqs. (2) and (3). However, the approximation given by Eq. (8) seems reasonable in view of the limited data that are available.

The specific application of Eq. (8) to the case of a flexible cable can be derived easily. If the cable of length L has the natural frequency (in water) f_n in the nth natural mode, then the wave length λ of the vibration is

$$\lambda = \frac{L}{n} = \frac{1}{2f_n}\sqrt{\frac{\bar{T}}{m'}} \tag{9}$$

where $\bar{T}$ is the tension and m' is the virtual (physical + added) mass per unit length of the cable. The shear parameter $\bar{\beta}$ for a linear shear flow can be reduced to the form

$$\bar{\beta} = \frac{D}{V_M}\,\frac{dV}{dz} = \frac{D}{V_M}\,\frac{\Delta V}{\Delta z} = \left[\frac{D}{L}\right]\frac{\Delta V}{V_M} \tag{10}$$

when the length scale $\Delta\bar{z}$ is equal to L and ΔV is the current velocity difference between the two ends of the cable. Equation (8) then takes the form

$$\frac{\Delta\bar{z}_{2-1}}{\lambda}\left[\frac{\lambda}{D}\right] = \Delta\left(\frac{f_s}{f}\right)_{2-1}\frac{1}{St\,\bar{\beta}\left[\dfrac{V_M}{fD}\right]}.$$

and upon substituting Eqs. (9) and (10) this equation reduces to

$$\frac{\Delta \bar{z}_{2-1}}{\lambda} = 2\Delta\left(\frac{f_s}{f}\right)_{2-1}\left(\frac{L}{D}\,St^{-1}\left(\frac{\Delta V}{f_n D}\right)^{-1}\left(fD\sqrt{\frac{m'}{T}}\right)\right). \tag{11}$$

From Fig. 22, $\Delta\left(\frac{f_s}{f}\right)_{2-1} = 0.7$ for $2\bar{Y}/D = 0.2$ and for most practical purposes $St = 0.2$ to 0.22. These substitutions reduce Eq. (11) to

$$\frac{\Delta \bar{z}_{2-1}}{\lambda} = 6.67\left(\frac{L}{D}\right)\left(\frac{\Delta V}{f_n D}\right)\left(fD\sqrt{\frac{m'}{T}}\right). \tag{12}$$

The length of a cable $\Delta\bar{z}$, in wavelengths, over which the vortex shedding locks on in a shear flow can be estimated from Eq. (12) in terms of the difference in flow velocity ΔV between the ends of the cable, the vibration and natural frequencies f and f_n respectively, and the cable tension T and virtual mass m' per unit length. For a cable in a shear flow the natural frequency f_n can be reasonably estimated by

$$f_n \sim f_{SM} = St\left(\frac{V_M}{D}\right).$$

It is important to note that Eq. (12) is an approximation for use in making practical estimates. The vortex shedding and cable strumming phenomena for a bluff body in a shear flow are highly unsteady in nature, and any predictions made with the equations developed here should be viewed as approximate mean estimates of the extent of vortex shedding.

Some experimental evidence is available to suggest that moderate shear levels do not appreciably decrease the probability of vortex-excited oscillations when the structural damping is low. King (33) found in his model tests with slender, cantilevered cylinders in water that large-amplitude, resonant cross flow oscillations ($\bar{Y} = \pm 1$ to $1.5\ D$) were readily excited in the first bending mode when the aspect ratio $L/D = 52$. The vortex shedding was locked onto the vibration over much of the length of the structure which was placed in a shear flow with a steepness parameter of $\bar{\beta} = 0.01$ to 0.015 (see Fig. 14). Kwok and Melbourne (31) and Howell and Novak (35) found that lock-on was readily

obtained in boundary layer shear flows over lengths of $L = 9$ to 10 D with flexibly-mounted circular cylinders that were excited to cross flow displacement amplitudes of $\bar{Y} = 0.15$ to 0.25 D (see Figs. 11 and 15).

6. CONCLUDING REMARKS

6.1 Summary. The flow about stationary and vibrating bluff bodies in a shear flow has undergone increasingly intensive study during the past ten years. Bluff cylinders both circular and non-circular in cross-section have been utilized in both wind tunnel and water channel experiments conducted to investigate the susceptibility of structures to vortex-excited oscillations. Most of the experiments conducted to date with stationary cylinders have demonstrated that a cellular pattern of vortex shedding exists along the span of the body. Over each cell the vortex shedding frequency is constant, and constant values of the Strouhal number and the base pressure coefficient are obtained when a characteristic velocity scale (usually, the mid-span value) is employed. A most important finding from several of the studies conducted thus far is that lightly damped structures both circular and non-circular (square and D-section) in shape undergo large amplitude cross flow oscillations in linear and boundary layer type shear flows of air and of water.

Some experiments also have been conducted to investigate the effects of turbulence on the response of cylinders in a shear flow. In the case of a linear shear flow with high turbulence level it was observed that the critical Reynolds number for a stationary circular cylinder was reduced by a factor of ten as had been found for the related case of an incident uniform flow. The vortex-excited cross flow response of a circular cylinder was found to be insensitive to the level of incident turbulence when the damping of the structure was small enough to cause lock-on between the vortex shedding and vibration frequencies.

Several experiments have been conducted with long cables in a linear shear flow. Vibrations of the cable were observed to lock-in with the vortex shedding as in the case of uniform flow. The addition of arrays of attached masses to the cable significantly altered the character of the vortex shedding as compared to the bare cable.

6.2 *Recommendations* Many of the studies conducted thus far have been small scale experiments and have been limited to cylinders with small aspect ratios of length/diameter less than $L/D = 15$ to 20. The cellular structure of the vortex shedding is influenced strongly by the end conditions for cylinders with these relatively small values of L/D and so it is important to conduct experiments with cylinders of sufficient length to minimize the effects of the end boundaries. The results obtained from experiments such as these will be of particular importance in the design of long, flexible marine structures and cable arrays.

It is important also to investigate further the effects of incident shear on the cross flow response of lightly-damped structures in air and in water. The relatively few experiments conducted thus far have demonstrated that cylindrical structures undergo large-amplitude unsteady motions in shear flows when the critical incident flow velocity is exceeded and the damping is sufficiently small. However, more definitive bounds for and details of this fluid-structure interaction are required for applications in both wind engineering design of buildings and structures and ocean engineering design of structures and cable systems.

7. REFERENCES

1. E. Naudascher, (ed.), *Flow-Induced Structural Vibrations*, Springer: Berlin (1974).

2. E. Naudascher and D. Rockwell (eds.), *Symposium on Practical Experiences with Flow-Induced Vibrations*, Springer: Berlin (1981).

3. T. Sarpkaya, "Vortex-Induced Oscillations—A Selective Review", Transactions of ASME, Journal of Applied Mechanics, Vol. 46, 241-258 (1979).

4. O.M. Griffin and S.E. Ramberg, "Some Recent Studies of Vortex Shedding with Application to Marine Tubulars and Risers," Transactions ASME, Journal of Energy Resources Technology, Vol. 104, 2-13 (March 1982).

5. S.E. Ramberg, "The Influence of Yaw Angle upon the Vortex Wakes of Stationary and Vibrating Cylinders" NRL Memorandum Report 3822 (August 1978).

6. F.D. Masch and W.L. Moore, "Drag Forces in Velocity Gradient Flow," Proceedings of the ASCE, Journal of the Hydraulics Division, Vol. 86, No. Hy 7, 1-11 (1960).

7. M.R. Starr, "The Characteristics of Shear Flows Past a Circular Cylinder," Ph.D. Thesis, University of Bristol: Bristol, U.K. (1966).

8. T.L. Shaw and M.R. Starr, "Shear Flows Past a Circular Cylinder," Proceedings of the ASCE, Journal of the Hydraulics Division, Vol. 98, No. Hy 3, 461-473 (1972).

9. D.J. Maull and R.A. Young, "Vortex Shedding From a Bluff Body in a Shear Flow," in *Flow-Induced Structural Vibrations*, E. Naudascher (ed.), 717-729 (1974).

10. D.J. Maull and R.A. Young, "Vortex Shedding From Bluff Bodies in a Shear Flow," Journal of Fluid Mechanics, Vol. 60, 401-409 (1973).

11. W.A. Mair and P.K. Stansby, "Vortex Wakes of Bluff Cylinders in a Shear Flow," SIAM Journal of Applied Mathematics, Vol. 28, 519-540 (1975).

12. F. Etzold and H. Fiedler, "The Near-Wake Structure of a Cantilevered Cylinder in a Cross-Flow," Zeitschrift fur Flugwissenshaften, Vol. 24, 77-82 (1976).

13. C. Fiscina, "An Investigation Into the Effects of Shear on the Flow Past Bluff Bodies," M.S. Thesis, University of Notre Dame: Notre Dame, Indiana (May 1977).

14. C. Fiscina, "An Experimental Investigation of the Flow Field Around a Bluff Body in a Highly Turbulent Shear Flow," Ph. D. Dissertation, University of Notre Dame: Notre Dame, Indiana (May 1979).

15. P.K. Stansby, "The Locking-on of Vortex Shedding Due to the Cross-Stream Vibration of Circular Cylinders in Uniform and Shear Flows," Journal of Fluid Mechanics, Vol. 74, 641-667 (1976).

16. B.J. Vickery and A.W. Clark, "Lift or Across-Wind Response of Tapered Stacks," Proceedings of ASCE, Journal of the Structural Division, Vol. 98, No. ST1, 1-20 (1972).

17. M.E. Davies, "The Effects of Turbulent Shear Flow on the Critical Reynolds Number of a Circular Cylinder," National Physical Laboratory (U.K.) NPL Report Mar Sci R 151 (January 1976).

18. O.M. Griffin, "A universal Strouhal number for the 'locking-on' of vortex shedding to the vibrations of bluff cylinders," Journal of Fluid Mechanics, Vol. 85, 591-606 (1978).

19. O.M. Griffin, "Universal similarity in the wakes of stationary and vibrating bluff bodies," Transactions of ASME, Journal of Fluids Engineering, Vol. 103, 52-58 (March 1981).

20. R.D. Peltzer and D.M. Rooney, "Effect of Upstream Shear and Surface Roughness on the Vortex Shedding Patterns and Pressure Distributions Around a Circular Cylinder in Transitional Re Flows," Virginia Polytechnic Institute and State University Report No. VIP-Aero-110 (April 1980).

21. J.A. Peterka, J.E. Cermak and H.G.C. Woo, "Experiments on the Behavior of Cables in a Linear Shear Flow" Fluid Mechanics and Wing Engineering Program, Colorado State University, Progress Report on Contract No. N68305-78-C-0055 for the Naval Civil Engineering Laboratory, Port Hueneme, CA. (May 1980).

22. H.G.C. Woo, J.A. Peterka and J.E. Cermak, "Experiments on Vortex Shedding from Stationary and Oscillating Cables in a Linear Shear Flow," Fluid Mechanics and Wind Engineering Program, Colorado State University, Final Report on Contract N68305-78-C-0055 for the Naval Civil Engineering Laboratory (July 1981).

23. R.D Peltzer and D.M. Rooney, "Vortex Shedding, Base Pressure and Wake Measurements Behind High Aspect Ratio Cylinders in Subcritical Reynolds Number Shear Flow," Final Report on NRL Contract No. N00173-80-C-0211, Virginia Polytechnic Institute and State University (February 1981); see also ASME Paper 81-WA/FE (November 1981).

24. S.J. Elsner, "A Critical Investigation of the Universal Strouhal Number for a Bluff Body in a Linear Shear Flow," M.S. Thesis, University of Notre Dame: Notre Dame, Indiana (June 1982).

25. R.D. Peltzer, "Vortex Shedding From a Vibrating Cable with Attached Spherical Bodies in a Linear Shear Flow," Ph.D. Thesis, Virginia Polytechnic Institute and State University: Blacksburg, VA (August 1982).

26. M. Kiya, H. Tamura and M. Arie, "Vortex-shedding from a circular cylinder in moderate-Reynolds-number shear-flow, Journal of Fluid Mechanics, Vol. 101, 721-736 (1980).

27. G. Buresti and A. Lanciotti, "Vortex Shedding From Smooth and Roughened Circular Cylinders in Cross Flow Near a Plane Surface," Aeronautical Quarterly, Vol. 28, 305-321 (February 1979).

28. N. Alemdaroglu, J.C. Rebillat and R. Goethals, "An Aeroacoustic Coherence Function Method Applied to Circular Cylinder Flows," Journal of Sound and Vibration, Vol. 69, 427-440 (1980).

29. E. Szechenyi, "Supercritical Reynolds number simulation for two-dimensional flow over circular cylinders," Journal of Fluid Mechanics, Vol. 70, 529-542 (1975).

30. A. Roshko, "On the development of turbulent wakes from vortex streets," NACA Report 1191 (1954).

31. K.C.S. Kwok and W.H. Melbourne, "Cross-Wind Response of Structures Due to Displacement Dependent Lock-in Excitation," in *Wind Engineering*, J.E. Cermak (ed.), Vol. 2, Pergamon: Oxford, 699-708 (1980).

32. F.J. Fischer, W.T. Jones and R. King, "Current-Induced Oscillation of Cognac Piles During Installation-Prediction and Measurements," in *Practical Experiences with Flow-Induced Vibrations*, E. Naudascher and D. Rockwell (eds.), Springer: Berlin, 570-581 (1980).

33. R. King, "Model Tests of Vortex Induced Motion of Cable Suspended and Cantilevered Piles for the Cognac Platform," BHRA Fluid Engineering Report RR 1453 (January 1978).

34. O.M. Griffin, "OTEC Cold Water Pipe Design for Problems Caused by Vortex-Excited Oscillations," Naval Research Laboratory Memorandum Report 4157 (March 1980).

35. J.F. Howell and M. Novak, "Vortex Shedding from Circular Cylinders in Turbulent Flow," in *Wind Engineering*, J.E. Cermak (ed.), Vol. I, 619-630 (1980); see also J.F. Howell, "Soil-Structure Interaction Under Wind Loading," Ph.D. Thesis, University of Western Ontario: London, Ontario (April 1978).

36. J. Cermak (ed.), *Wind Engineering, Proceedings of the Fifth International Conference on Wind Engineering*, Pergamon: Oxford (1980).

37. K.J. Eaton (ed.), *Proceedings of the Fourth International Conference on Wind Effects on Buildings and Structures*, Cambridge University Press: Cambridge, UK (1976).

38. J.K. Vandiver and O.M. Griffin, "Measurements of the Vortex-Excited Strumming Vibrations of Marine Cables," Ocean Structural Dynamics Symposium '82 Preprints, Oregon State University, September 1982.

39. O.M. Griffin, R.A. Skop and S.E. Ramberg, " The Resonant, Vortex-Excited Vibrations of Structures and Cable Systems." Offshore Technology Conference Preprint 2319 (1975).

40. R.A. Skop and O.M. Griffin, "On a Theory for the Vortex-Excited Oscillations of Flexible Cylindrical Structures," Journal of Sound and Vibration, Vol. 41, 263-274 (1975).

41. O.M. Griffin, "Vortex-Excited Cross Flow Vibrations of a Single Cylindrical Tube," in *Flow-Induced Vibrations*, S.S. Chen and M.D. Bernstein (eds.), ASME: New York, 1-10 (June 1979); see also Transactions of ASME, Journal of Pressure Vessel Technology, Vol. 102, No. 2, 158-166 (1980).

42. O.M. Griffin, S.E. Ramberg, R.A. Skop, D.J. Meggitt and S.S. Sergev, "The Strumming Vibrations of Marine Cables: State-of-the-Art," Naval Civil Engineering Laboratory Technical Note N-1608 (May 1981).

43. R.B. Dean, R.W. Milligan and L.R. Wootton, "An Experimental Study of Flow-Induced Vibration" E.E.C. Report 4, Atkins Research and Development Ltd.: Epsom, U.K. (1977).

44. E. Simiu and R.A. Scanlan, *Wind Effects on Buildings and Structures: An Introduction to Wind Engineering*, Wiley-Interscience: New York (1978).

45. O.M. Griffin, "Steady Hydrodynamic Loads due to Vortex Shedding from the OTEC Cold Water Pipe," NRL Memorandum Report 4698 (January 1982).

46. M.J. Every, R. King and O.M. Griffin, "Hydrodynamic Loads on Flexible Marine Structures Due to Vortex Shedding," Transactions of ASME, Journal of Energy Resources Technology, Vol. 104, in press (December 1982); see also ASME Paper 81-WA/FE-24 (November 1981).

47. M.J. Every, R. King and D.S. Weaver, "Vortex Excited Oscillations of Cables and Cylinders and Their Suppression," Ocean Engineering, Vol. 9, No. 2, 135-158 (1982).

48. D. Meggitt, J. Kline and J. Pattison, "Suppression of Mooring Cable Strumming," Proceedings of the Eighth Ocean Energy Conference, Paper IB5, Marine Technology Society: Washington, DC, (September 1982).

8. APPENDIX: METHODS FOR ESTIMATING THE CROSS FLOW OSCILLATIONS OF OSCILLATIONS OF FLEXIBLE CABLES AND STRUCTURES

General procedures. Design procedures and prediction methods for analyzing the vortex-excited oscillations of structures in water and in air have been developed only since the mid 1970's. Previously a reliable experimental data base and accurate characterization of the phenomenon were relatively unavailable, and it has been only since marine construction has moved into deeper water and more harsh

operating environments that the need for sophisticated design procedures has arisen. The need to design tall, slender structures against problems due to vortex shedding in the atmospheric environment also has spurred renewed efforts to develop new wind engineering design procedures. It should be emphasized, however, that reliable data are available only at subcritical Reynolds numbers. The design procedures that are generally available have been discussed recently in two related NRL and NCEL reports (34,42).

All of the methods developed thus far are in common agreement that the following parameters determine whether large-amplitude, vortex-excited oscillations are likely to occur:

- The *logarithmic decrement* of *structural* damping, δ
- The reduced velocity, $V/f_n D$;
- The mass ratio, $m_e/\rho D^2$.

Here m_e is the *effective mass* of the structure which is defined as

$$m_e = \frac{\int_0^L m(z)y^2(z)\,dz}{\int_0^h y^2(z)\,dz} \tag{A.1}$$

where $m(z)$ is the cylinder mass per unit length including internal water or other fluid and the added mass, joints, sections of different material, etc.; $y(z)$ is the modal shape of the structure along its length; L is the overall length of the structure, measured from its termination; h is the water depth. It should be noted here that many of these methods were developed originally for structural members that pierced the water surface, hence the length L was greater than the depth h. The effective mass m_e then defines an equivalent structure whose vibrational kinetic energy is equal to that of the real structure.

As described in references 34 and 42, the mass parameter and the structural damping can be combined as

$$k_s = \frac{2m_e\delta}{\rho D^2} \text{ or } \frac{\zeta_s}{\mu} = 2\pi St^2 k_s \tag{A.2}$$

which in both forms are called the reduced damping. The reduced damping k_s is the ratio of the actual damping *force* (per unit length) and the quantity $\rho f_n D^2$, which can be viewed as an inertial force. Available results also suggest criteria for determining the critical incident flow velocities for the onset of vortex-excited motions. These critical velocities are

$$V_{crit} = (f_n D) V_{r,crit} \tag{A.3}$$

where $V_{r,crit} = 1.2$ for in line oscillations and $V_{r,crit} = 3.5$ for cross flow oscillations at Reynolds numbers greater than about 5×10^5. For Reynolds numbers below 10^5, $V_{r,crit} = 5$.

It was noted above that the peak cross flow displacement amplitude is a function primarily of a response or reduced damping parameter when the damping is small and $\zeta_s = \delta/2\pi$. The importance of the reduced damping follows directly from resonant force and energy balances on the vibrating structure. Moreover, the relation between Y_{MAX} ($Y = \bar{Y}/D$) and k_s or ζ_s/μ holds equally well for flexible cylindrical structures with normal mode shapes given by $\psi_i(z)$, for the i th mode. If the cross flow displacement (from equilibrium) of a flexible structure is written as (34)

$$y_i = Y \psi_i(z) \sin \omega t$$

at each spanwise location z, then the peak displacement is scaled by the factor

$$Y_{EFF,MAX} = Y I_i^{1/2} / |\psi_i(z)|_{MAX} = Y_i/\gamma_i \tag{A.4}$$

In this equation

$$I_i = \frac{\int_0^L \psi_i^4(z)\, dz}{\int_0^L \psi_i^2(z)\, dz}$$

and

$$\gamma_i = \frac{|\psi_i(z)|_{MAX}}{I_i^{1/2}}$$

which are derived from considerations based on several related versions of the so-called "wake oscillator" formulation for predicting vortex-excited oscillations. Typical values of γ_i, ψ_i and I_i are tabulated in references 31 and 41. Cable applications specifically are discussed by Griffin et al. (42).

Step-by-step procedures for determining the deflections that result from vortex-excited oscillations have been developed by several groups, and these procedures are summarized in reference 34. The steps to be taken generally should follow the sequence:

- Compute/measure vibration properties of the structure (natural frequencies or periods, normal modes, modal scaling factors, etc.)

- Compute Strouhal frequencies and test for critical velocities, V_{cr_n} (in line and cross flow), based upon the incident flow environment.

- Test for reduced damping, k_s, based upon the structural damping and mass characteristics of the structure.

  If the structure is susceptible to vortex-excited oscillations, then

- Determine vortex-excited unsteady displacement amplitudes and corresponding mean deflections based upon the steady drag amplification that accompanies the oscillations.

- Determine new cumulative stress distributions based upon the new steady-state deflection and the superimposed forced mode shape induced by the unsteady forces, displacements and accelerations that accompany the vortex shedding.

- Assess the severity of the amplified stress levels relative to fatigue life, critical stresses, etc.

These general procedures are discussed in detail in reference 34 where several practical design problems also are given as examples. Kwok and Melbourne (31) discuss applications to wind engineering design of structures from an empirical viewpoint, and Simiu and Scanlan (44) discuss applications of the wake-oscillator type of approach to applications in wind engineering. Examples of the predicted drag-induced steady deflections due to vortex-excited oscillations are compared with experimental results by Griffin (45) and by Every, King and Griffin (46). Good agreement was obtained between the predicted deflections and measurements on a flexible cantilever beam described by King (33).

An increase in the reduced damping results in smaller amplitudes of oscillation and at large enough values of ζ_s/μ or k_s the vibratory motion becomes negligible. Reference to Fig. 24 suggests that oscillations are effectively suppressed at $\zeta_s/\mu > 4$ (or $k_s > 16$). Cylindrical structures in water fall well toward the left-hand portion of the figure. The measurements of in line oscillations in water have shown that vortex-excited motions in that direction are effectively negligible for $k_s > 1.2$. The results obtained by Dean, Milligan and Wootton (43), King (33) and others shown in Fig. 24 indicate that the reduced damping can increase from $\zeta_s/\mu = 0.01$ to 0.5 (a factor of *fifty*) and the peak-to-peak displacement amplitude is decreased only from 2 or 3 diameters to 1 diameter (a nominal factor of only *two or three*). At the small mass ratios and structural damping ratios that are typical of light, flexible structures in water, the hydrodynamic forces predominate and it is difficult to reduce or suppress the oscillations by changing the mass and damping of the structure.

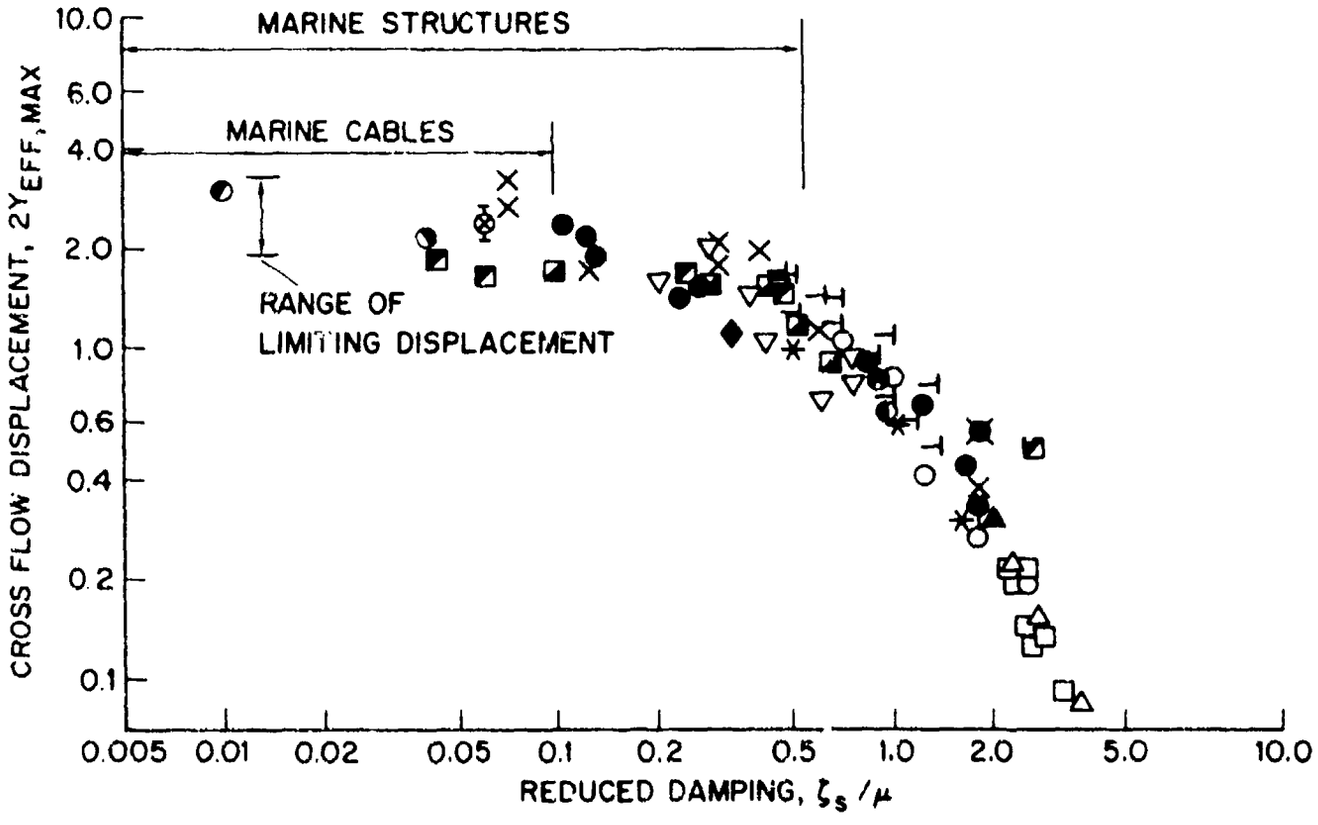

Figure 24. Maximum vortex-excited cross flow displacement amplitude $2Y_{EFF,MAX}$ of circular cylinders, scaled as in equation (A.4), plotted against the reduced damping $\zeta_s/\mu = 2\pi St^2(2m\delta/\rho D^2)$. The legend for the data points is given in Table A1

Thus it now is possible to adequately predict the material stresses and deflections that are caused by the vortex-excited oscillations of cables and bluff structures. Every, King and Griffin (46) also discuss some devices for the suppression of vortex-excited oscillations that have been employed successfully in offshore engineering applications. Every, King and Weaver (47) and Meggitt, Kline and Pattison (48) give extensive discussions of the various devices that have been developed and tested specifically for cable strumming suppression

Table A1. Vortex-excited cross flow displacement amplitude response of cylindrical structures.

Legend for Data Points in Fig. 24	
Type of cross-section and mounting: medium	Symbol
Various investigators, from Griffin (41):	
Spring-mounted rigid cylinder; air	* ○ ⊣ ■ ◐
Spring-mounted rigid cylinder; water	◆
Cantilevered flexible circular cylnider; air	△
Cantilevered flexible circular cylinder; water	× ▽ ○
Pivoted rigid circular rod; air	□ ▲
Pivoted rigid circular rod; water	●
From Dean, Milligan and Wootton (43):	
Spring-mounted rigid cylinder; water	◩
Flexible circular cylinder, L/D = 72; water	◪
From King (33):	
Cantilevered flexible circular cylinder, L/D = 66 (PVC); water	◕
Cantilevered flexible circular cylinder, L/D = 66 (Stainless steel); water	◐